

Supporting Information

Nano Au/Pd catalyzed ‘on-water’ synthesis of C3-C3’ diaryl -oxindole scaffolds via N2-selective dearomatization of indole

Shivanee Borpatra Gohain,^a Monika Basumatary,^b Purna K. Boruah^{c,d}, Manash R. Das^{c,d} and Ashim Jyoti Thakur^{*a}

^{a.} *Dept. Of Chemical Sciences, Tezpur University, Napaam 784028, Assam, INDIA*

^{b.} *Phytochemistry Division. Defence Research Laboratory, Solmara, Tezpur 784001.*

^{c.} *Advance Materials Group, Materials Sciences and Technology Division, CSIR-North East Institute of Sciences and Technology, Jorhat, Assam, India*

^{d.} *Academy of Scientific and Innovative Research, CSIR-NEIST Campus, India*

List of contents

(1) General Experimental Methods.....	S2
(2) Preparation of the catalysts.....	S2
(3) Characterization of the catalysts.....	S3
(4) General synthetic procedures.....	S4
(5) Recycling potential of nanocatalysts.....	S4
(6) List of figures.....	S5
(7) List of tables.....	S14
(8) Physical and Spectroscopic Data of Compounds.....	S17
(9) ^1H NMR and ^{13}C NMR spectra of compounds.....	S20
(10) List of selected previous works.....	S37
(11) Crystallographic data and molecular structure of compound 8c	S38
(12) NOE NMR of compound 8c	S39
(13) References.....	S40

(1) General Experimental Methods:

The chemicals and reagents were purchased from Sigma-Aldrich, Merck, Alfa Aesar and Loba chemical, and used without further purification. Melting points were determined in a Büchi 504 apparatus. ^1H and ^{13}C NMR spectra were recorded in a 400 MHz NMR spectrophotometer (JEOL, JNM ECS) using tetramethylsilane (TMS) as the internal standard and coupling constants are expressed in Hertz. Visualization was accomplished with UV lamp or I_2 stain. Reactions were monitored by thin-layer chromatography using aluminium sheets with silica gel 60 F₂₅₄ (Merck). The products were isolated by column neutral alumina using EtOAc:Hexane(30%)as an eluent.

(2) Preparation of the catalysts:

Synthesis of graphene oxide (GO)

The synthesis of GO is carried out using modified Hummer's method.¹

Synthesis of Pd NPs supported on reduced graphene oxide(rGO) (Pd-rGO nanocomposite) (Using microwave)

For the preparation of Pd/rGO, 0.1 g of the dried GO and palladium acetate (0.1g in 10 wt.% HNO_3 , 99.999%) were sonicated in deionized water until a homogeneous yellow dispersion was obtained. The solution was placed inside a conventional microwave after adding 100 micro litre of the reducing agent, hydrazine hydrate (HH). The microwave oven then operated at power (300 W) for 40s. The yellow solution of Pd-GO changed to a black colour, indicating the formation of NPs and *in-situ* chemical reduction to rGO. In order to separate the Pd-rGO sheets, water (20

mL) was added to the solution and centrifuged by using Eppendorf centrifuge operated at 5000 rpm for 15 min and dried overnight under vacuum.²

Synthesis of Pd NPs supported on rGO(Pd-rGO nanocomposite) (Without using microwave)

The above-mentioned method is carried out till addition of reducing agent followed by stirring at room temperature for 28 hours. The Pd-rGO sheets were further separated by using Eppendorf centrifuge operated at 5000 rpm for 15 min and dried overnight under vacuum.

Synthesis of Au NPs (Citrate Reduction Method)

100 mL of 10^{-2} M HAuCl₄ was brought to a reflux while stirring and then 10 mL of a 38.8 mM trisodium citrate solution was added quickly, which resulted in a slight colour change of the solution from pale yellow to light purple. After the colour changed, the solution was refluxed for 6 hrs. The colour of the solution was turned to deep purple colour. An additional 4 hours of reflux showed no difference in colour. The solution was refluxed for total 10 hours at a temperature of about 80 °C at rpm of 1000-1500.³

Synthesis of Au-Pd NPs supported on rGO (Au-Pd-rGO nanocomposite)

For the preparation of Au-Pd-rGO, 0.1 g of the dried GO, Pd(OAc)₂ (0.1g in 10 wt.% HNO₃, 99.999%) and HAuCl₄ (0.005g) were sonicated in deionized water until a homogeneous yellow dispersion was obtained. The solution was placed inside a conventional microwave after adding 100 micro litre of the reducing agent, hydrazine hydrate (HH). The microwave oven then operated at power (300 W) for 40s. The yellow solution of Au-Pd-GO changed to a black colour, indicating the formation of the catalyst. In order to separate the Au-Pd-rGO sheets, water (20 mL) was added to the solution and centrifuged by using Eppendorf centrifuge operated at 5000 rpm for 15 min and dried overnight under vacuum.

Synthesis of Au@Pd core-shell NPs

For the preparation of Au@Pd core-shell NPs, Pd(OAc)₂ (0.1g in 10 wt.% HNO₃, 99.999%) and HAuCl₄(0.005g) were sonicated in deionized water until a homogeneous yellow dispersion was obtained. The solution was placed inside a conventional microwave after adding 100 micro litre of the reducing agent, hydrazine hydrate (HH). The microwave oven then operated at power (300 W) for 40s. The yellow solution of changed to a black colour, indicating the formation of the catalyst.

(3) Characterization of the catalysts:

The FESEM images of GO, Pd-rGO and Au-Pd-rGO are shown in figure 3 (iv) (manuscript). Spherical particles of well-ordered surface morphology are observed in the FESEM picture of the sample. EDX analyses were performed to determine the elemental constituents of Pd-rGO nanocomposite and Au-Pd-rGO (Table 1, manuscript and Fig. S10, ESI). It showed that the weight% of Pd was found to be 16.2% in Pd-rGO and atomic % of Pd and Au in Au-Pd-rGO was

20.82 and 0.34 respectively. Thus, the EDX suggests the presence of only Pd in Pd-rGO, and Pd and Au in the Au-Pd-rGO sample respectively.

The BET surface area of Pd-rGO was found to be $77.120\text{ m}^2\text{g}^{-1}$.

The X-ray diffractograms were obtained (XRD, MINI FLEX RIGAKU MODEL) with Cu K- α radiation (1.5418 \AA) with scanning rate of 2° per min from 2° to 80° . The X-ray diffraction spectrum (XRD) of the nanocatalysts is shown in Fig. S5 (ESI).

(4) General synthetic procedures

(A) General Procedure for the synthesis of 2,2-Bis(indolyl-3-yl)indoline-3-ones:

In an oven dried round bottomed flask (50 mL) nanocatalyst and solvent (2 ml) was added followed by indole (0.0586 g, 0.5 mmol) and oxone (0.3805 g, 0.25 mmol). After that it was allowed to stir on a pre heated oil bath till the required time (the progress of the reaction was judged by TLC). The reaction mixture was brought to room temperature after its completion and ethyl acetate ($3 \times 10\text{ mL}$) was added to it and then centrifuged at 3,500 rpm to recover the nano catalyst. Having done this, the reaction mixture was washed with water and brine, dried over Na_2SO_4 , concentrated in a rotary evaporator and finally the crude product was purified by column chromatography (30% ethyl acetate: hexane as an eluent).

(5) Recycling potential of nanocatalysts

After carrying out the experiment, ethyl acetate was poured and the reaction mixture was centrifuged to pellet out the Pd-rGO nanocomposite. The particles were then extracted by simple centrifugation (3,000 rpm) and washed with hot ethanol ($3 \times 10\text{ mL}$) to remove all the organic impurities. Finally it was decanted and dried in vacuum. The recovered nanocatalyst was used directly in the next cycle. The Pd-rGO nanocomposite was found to be equally effective up to 4th cycle (Fig. S9, ESI), and after that the product yield slightly decreases as shown in Fig. S10, ESI.

(6) List of figures

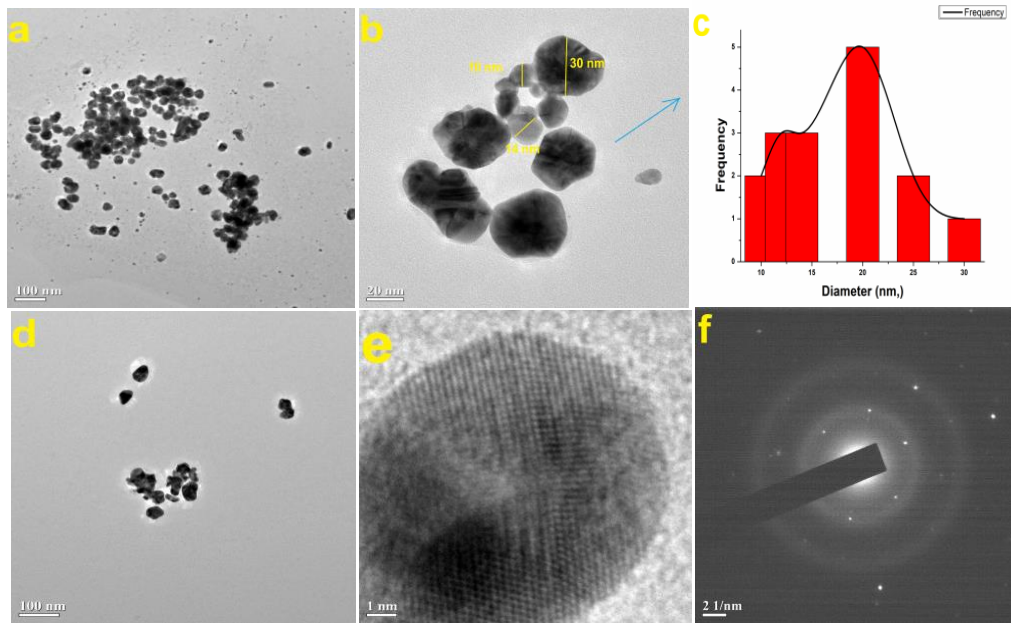


Fig. S1 (a, b, d) TEM images, (c) particle size distribution curve, (e) HRTEM image and (f) SAED pattern of Au NPs

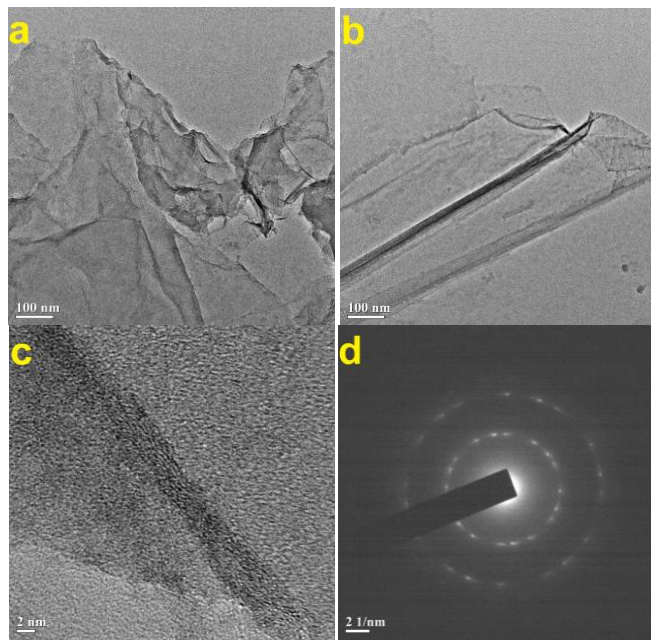
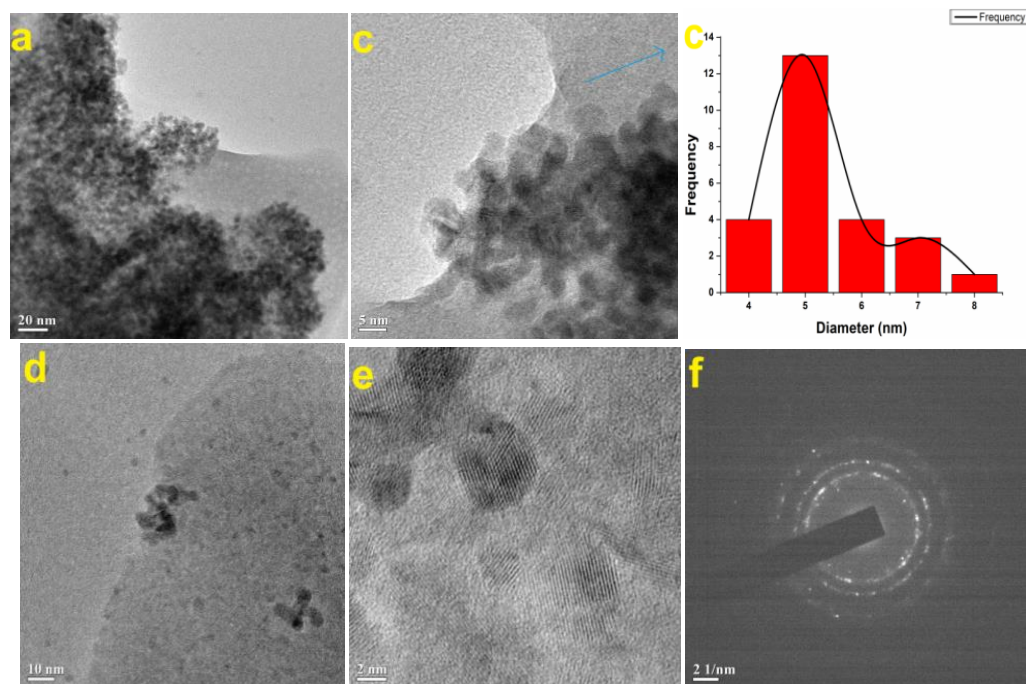
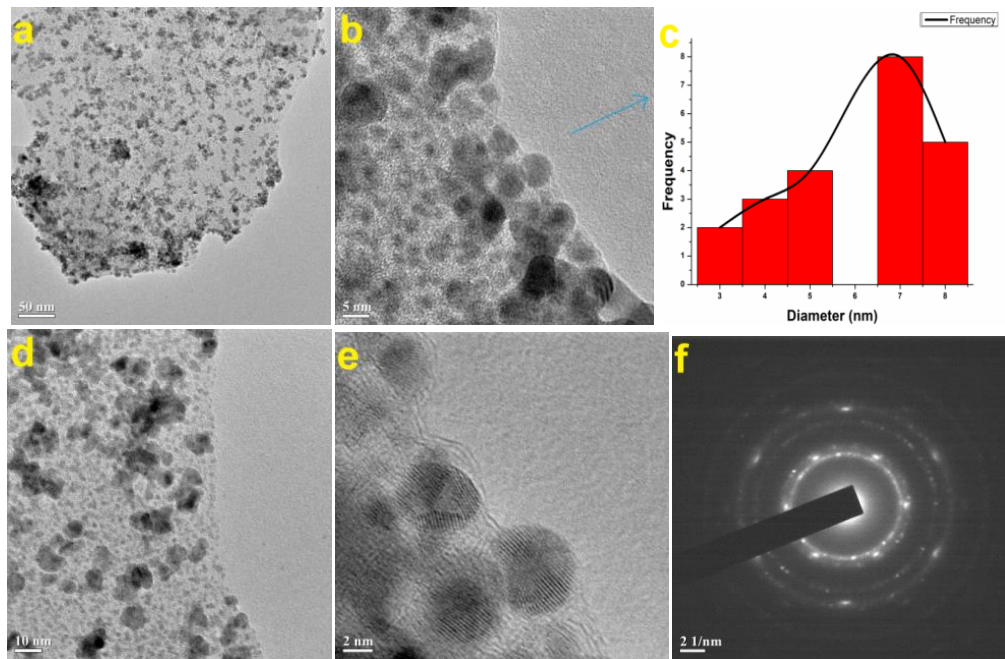


Fig. S2 (a, b, c) TEM images and (d) SAED pattern of graphene oxide (GO)



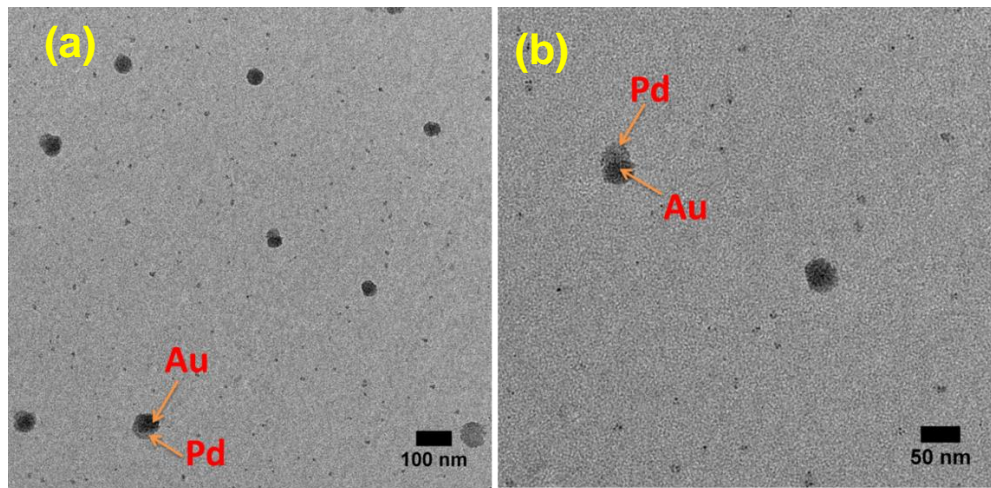


Fig. S5.. (a) TEM and (b) High-resolution TEM image displaying the Au@Pd core-shell NPs.

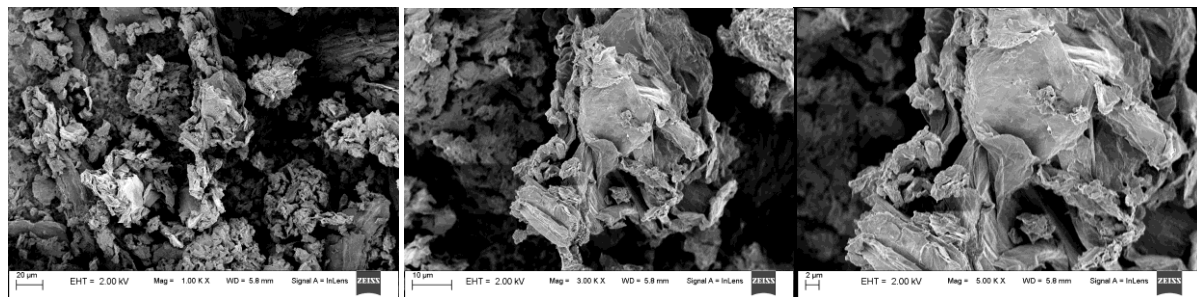


Fig. S6 FESEM images of GO

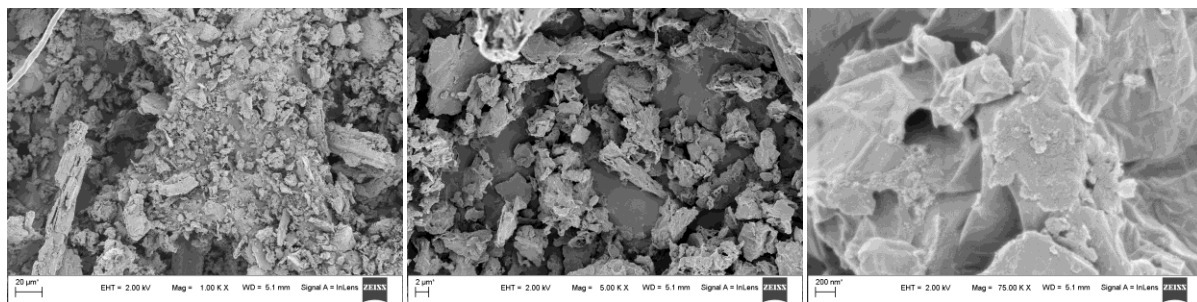


Fig. S7 FESEM images of Pd-rGO nanocomposite

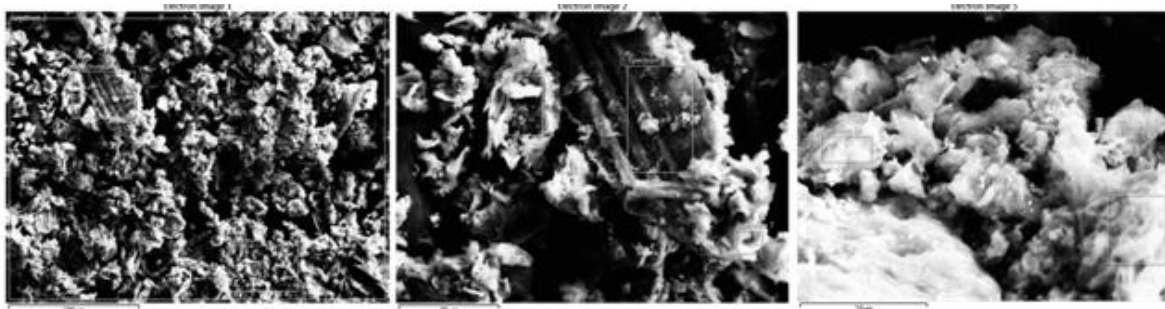


Fig. S8 FESEM images of Au-Pd-rGO nanocomposite

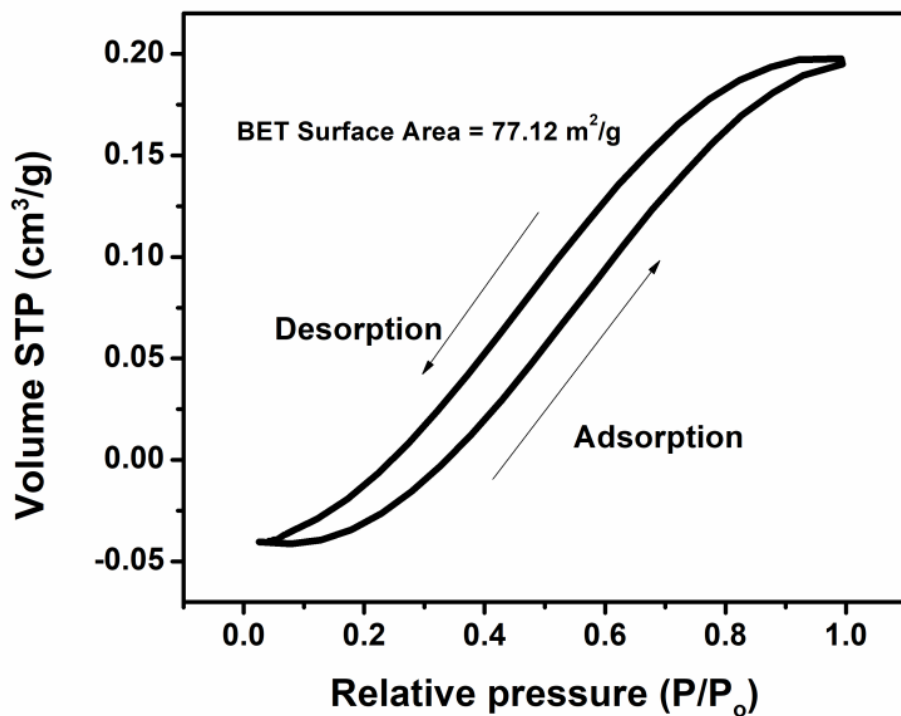


Fig. S9 Nitrogen adsorption isotherm of Pd-rGO nanocomposite

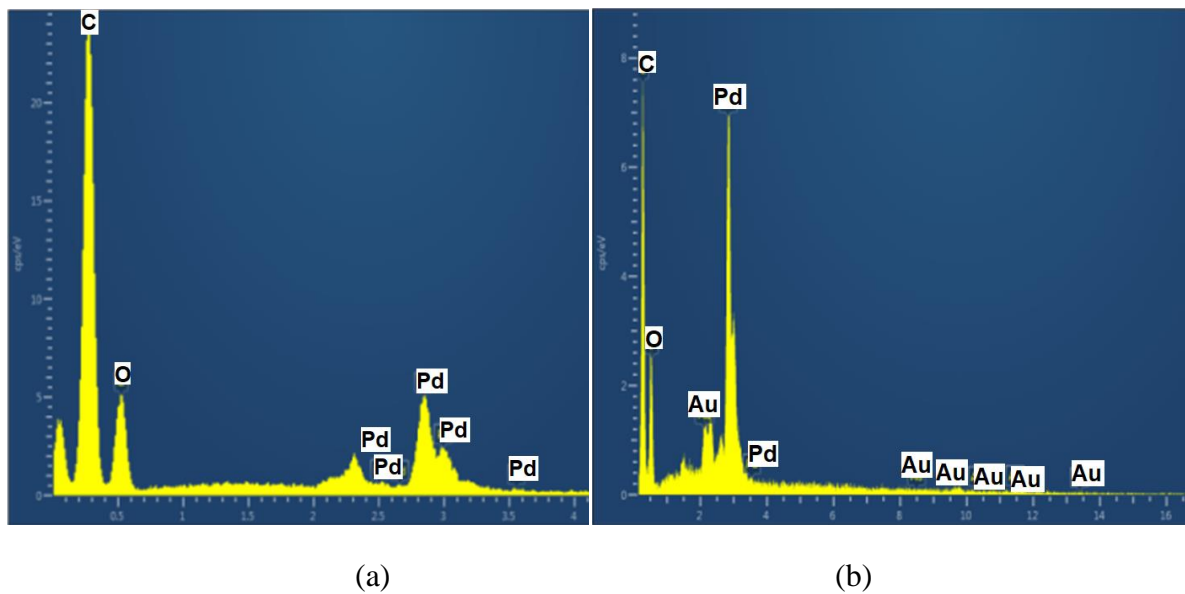


Fig. S10 EDX of (a) Pd-rGO nanocomposite and (b)Au-Pd-rGO nanocomposite

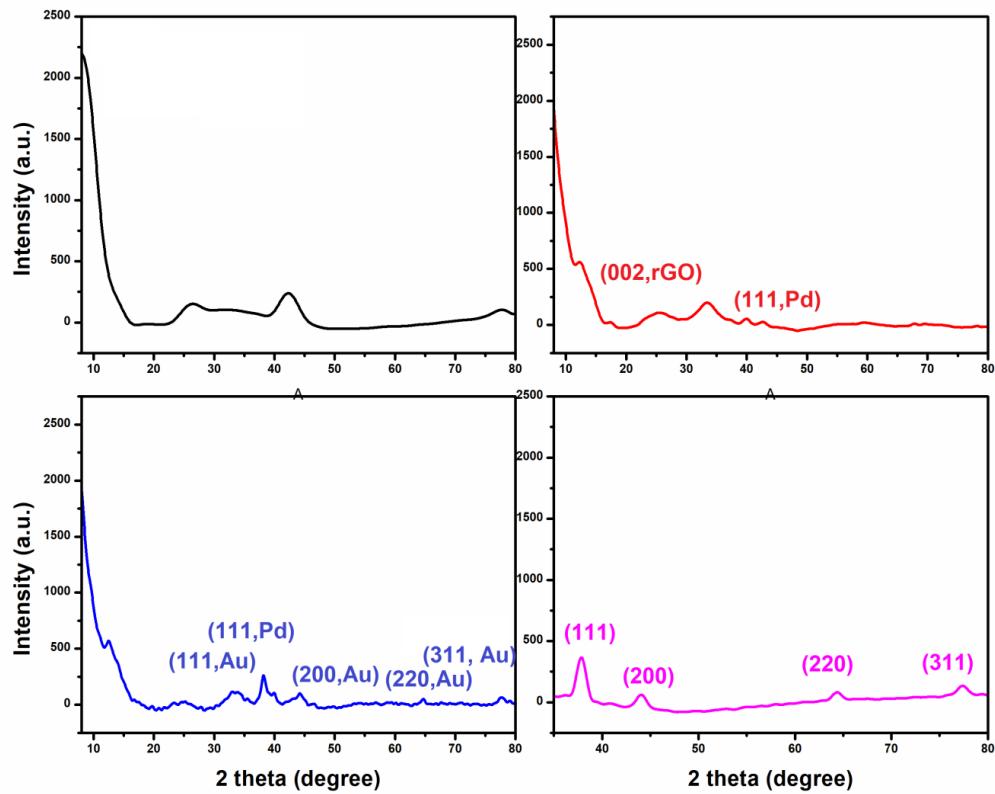


Fig. S11 PXRD plots of GO (black), Pd-rGO nanocomposite (red), Au-Pd-rGO nanocomposite (blue) and Au NPs (pink)

X-ray photoelectron spectroscopy (XPS) analysis was performed with an ESCALAB 220 XL spectrometer from Vacuum Generators featuring a monochromatic Al K α X-ray source (1486.6 eV) and a spherical energy analyzer operated in the (constant analyzer energy) mode (CAE=100 eV for survey spectra and 50 eV for high-resolution spectra), using the electromagnetic lens mode.

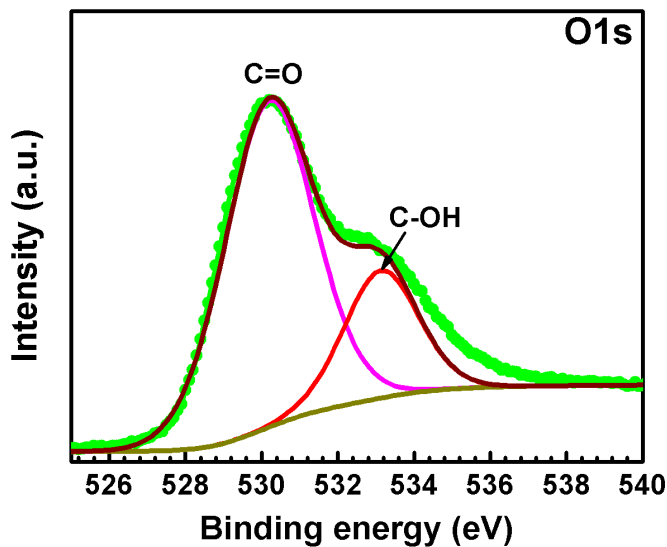


Fig. S12 High-resolution O1s XPS spectrum of Au-Pd-rGO

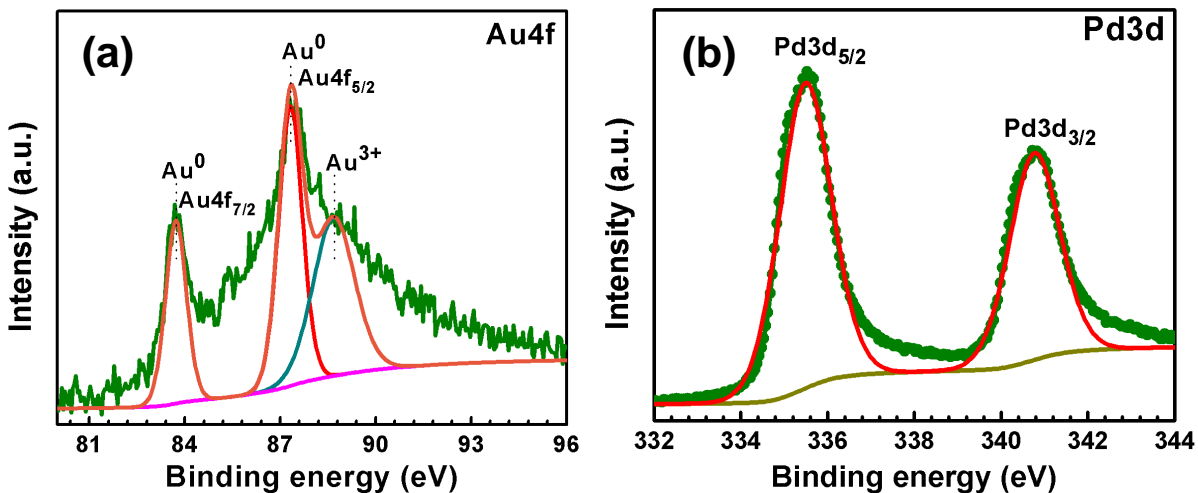


Fig. S13 High resolution XPS spectra of (a) Au4f and (b) Pd3d ofcore-shell Au-Pd NPs

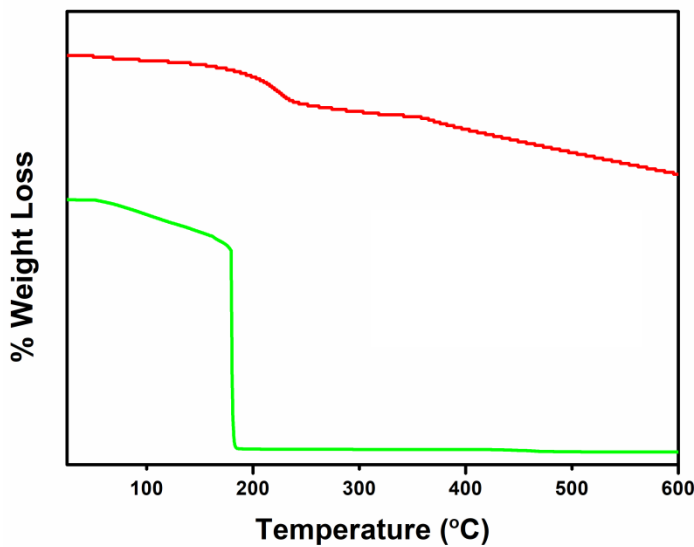


Fig. S14 TGA curve of GO (green) and Pd-rGO nanocomposite (red)

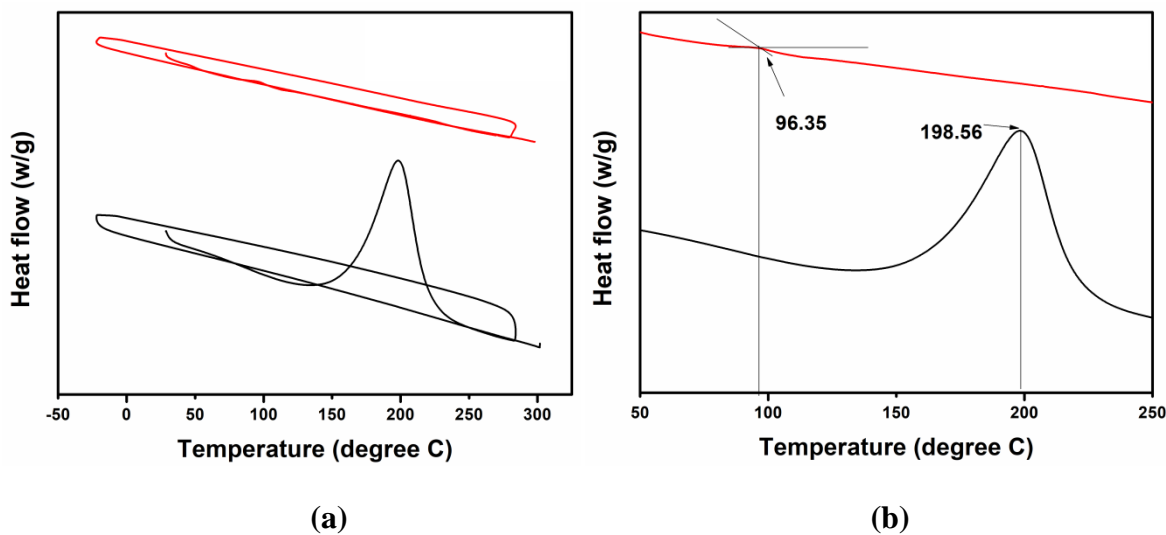


Fig. S15 DSC plots of (a) GO (black) and (b) Pd-rGO nanocomposite (red)

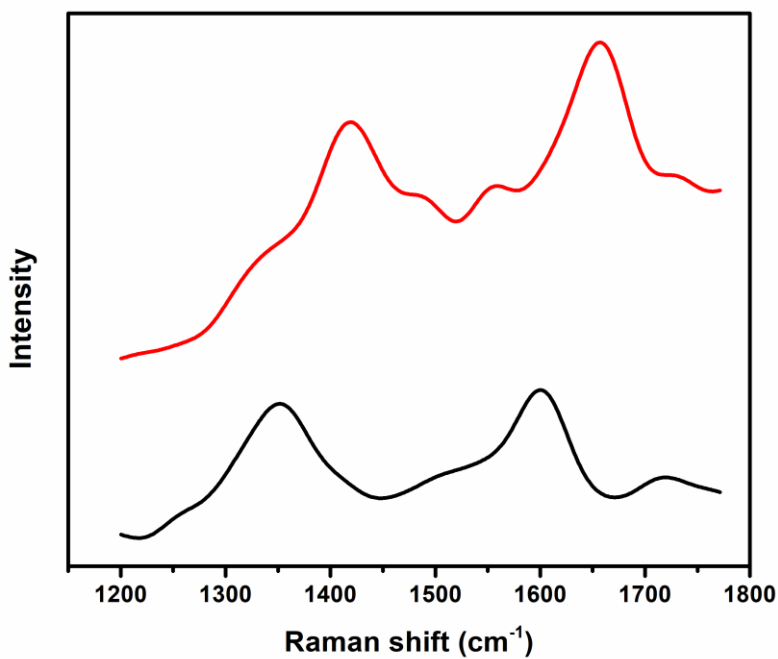


Fig. S16 Raman plots of Pd-rGO nanocomposite (black) and Au-Pd-rGO nanocomposite (red)

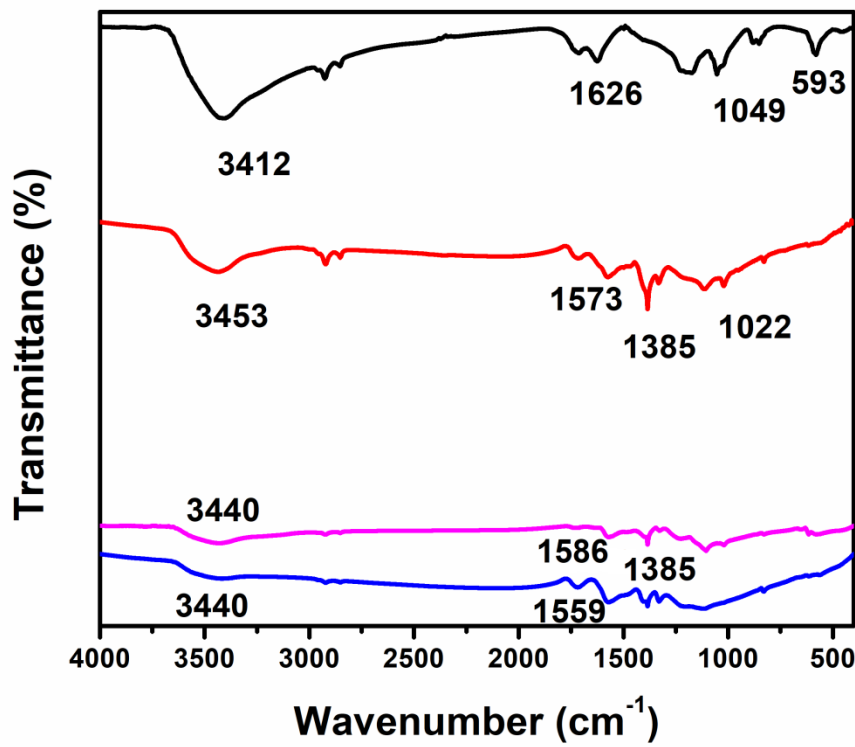


Fig. S17 FT-IR spectra of GO (black), Pd-rGO nanocomposite (Microwave) (red), Pd-rGO nanocomposite (No Microwave) (blue) and Au-Pd-rGO nanocomposite (pink)

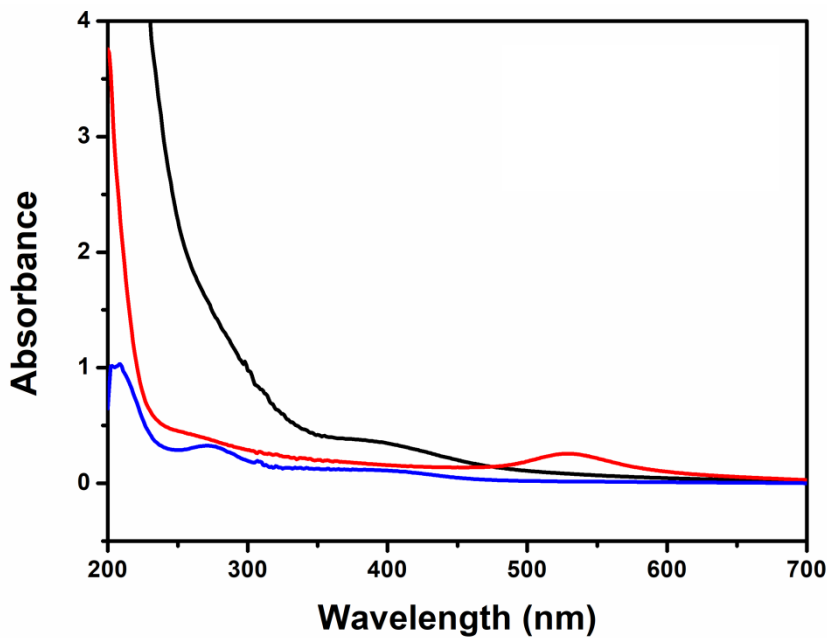


Fig. S18 UV-Vis spectra of Pd(OAc)₂(black), Pd-rGO nanocomposite (blue) and Au NPs (red)

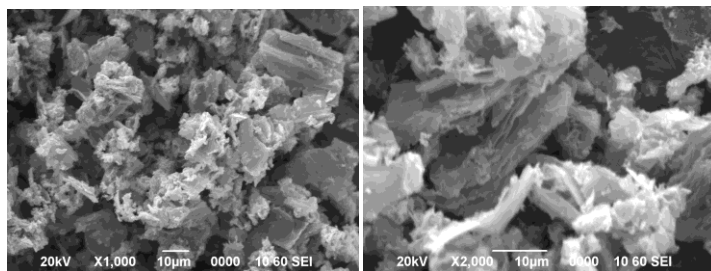


Fig. S19 SEM images of recycled Pd-rGO nanocomposite (after 4thcycle)

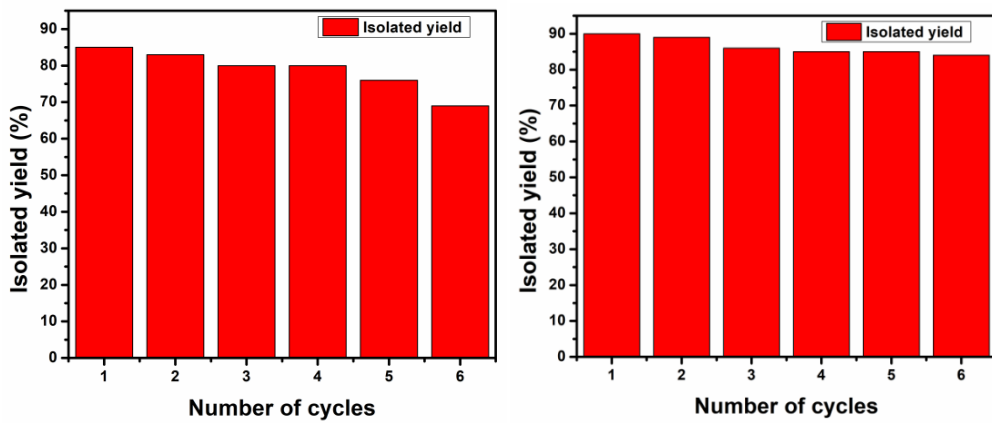
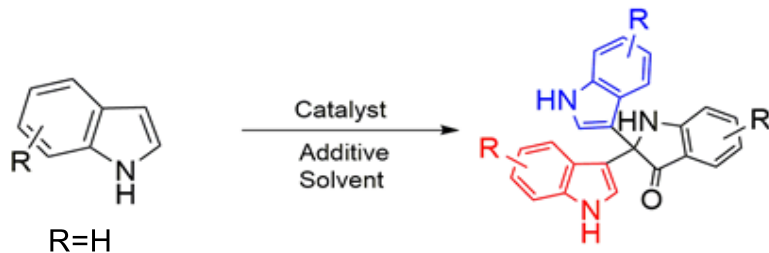


Fig. S20 Catalyst recyclability chart of Pd-rGO nanocomposite and Au-Pd-rGO nanocomposite

(7) List of tables

Table S1. Optimization reaction conditions^a with bulk and nano catalysts for synthesis of 2,2-Bis(indol-3-yl)indolin-3-ones (scheme 2)



Entry	Catalyst	Additive	Solvent	Time (h)	Yield (%) ^b
1 ^c	None	None	None	16	-
2 ^c	None	None	Toluene	16	-
3 ^c	Bulk Pd(OAc) ₂	None	Toluene	16	-
4 ^c	Bulk Pd(OAc) ₂	K ₂ CO ₃	Toluene	16	-
5 ^c	Bulk Pd(OAc) ₂	Na ₂ CO ₃	Toluene	16	-
6 ^c	Bulk Pd(OAc) ₂	Cs ₂ CO ₃	Toluene	16	-
7	Bulk Pd(OAc) ₂	Oxone	Toluene	16	10
8 ^c	Bulk HAuCl ₄	None	Toluene	16	-
9 ^c	Bulk HAuCl ₄	K ₂ CO ₃	Toluene	16	-
10 ^c	Bulk HAuCl ₄	Na ₂ CO ₃	Toluene	16	-
11 ^c	Bulk HAuCl ₄	Cs ₂ CO ₃	Toluene	16	-
12	Bulk HAuCl ₄	Oxone	Toluene	16	10
13	None	Oxone	Toluene	18	5
14 ^c	Pd-rGO	None	Toluene	16	-
15 ^c	Pd-rGO	K ₂ CO ₃	Toluene	16	-
16 ^c	Pd-rGO	Na ₂ CO ₃	Toluene	16	-
17 ^c	Pd-rGO	Cs ₂ CO ₃	Toluene	16	-
18	Pd-rGO	Oxone	Toluene	10	60
19 ^c	Au NPs	K ₂ CO ₃	Toluene	16	-
20 ^c	Au NPs	Na ₂ CO ₃	Toluene	16	-
21	Au NPs	Oxone	Toluene	12	54
22 ^c	Au-Pd-rGO	K ₂ CO ₃	Toluene	16	-
23 ^c	Au-Pd-rGO	Na ₂ CO ₃	Toluene	16	-
24 ^c	Au-Pd-rGO	Cs ₂ CO ₃	Toluene	16	-
25	Au-Pd-rGO	Oxone	Toluene	12	52

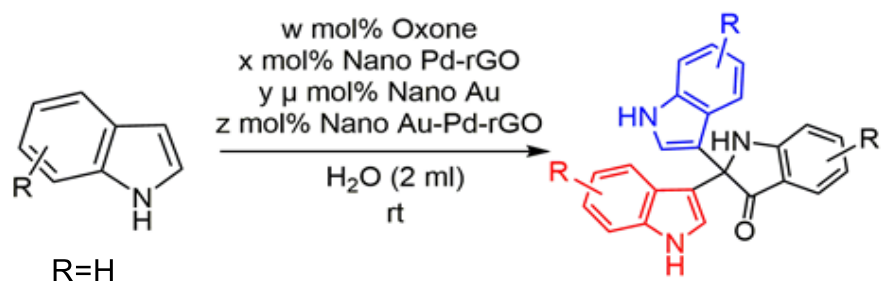
^aReaction conditions: Indole (0.5 mmol), additive (0.5 mmol), catalyst (0.5 mol%), solvent (2ml), 90 °C. ^bIsolated Yields. ^cNo reaction was observed.

Table S2. Optimization with different nanocatalysts for the reaction

Entry	Catalyst 1	Catalyst 2	Solvent	Temp. (°C)	Time (h)	Yield (%) ^b
1	Pd-rGO	None	Dioxane	90	8	65
2	Pd-rGO	None	DCM	90	8	60
3	Pd-rGO	None	DCE	90	8	65
4	Pd-rGO	None	DMF	90	8	60
5	Pd-rGO	None	THF	90	8	30
6	Pd-rGO	None	Methanol	90	8	40
7	Pd-rGO	None	Ethanol	90	8	40
8	Pd-rGO	None	Water	90	8	75
9	Pd-rGO	None	Neat	90	8	55
10	Au NPs	None	Dioxane	60	12	57
11	Au NPs	None	DCM	60	12	65
12	Au NPs	None	DCE	60	12	60
13	Au NPs	None	Ethanol	60	12	45
14	Au NPs	None	Methanol	60	12	30
15	Au NPs	None	Water	60	12	71
16	Pd-rGO	Au NPs	Dioxane	rt	3	65
17	Pd-rGO	Au NPs	Ethanol	rt	3	55
18	Pd-rGO	Au NPs	Water	rt	3	82
19	Pd-rGO	Au NPs	Neat	rt	3	55
20	Pd-rGO	None	Dioxane	rt	3	45
21	Au-Pd-rGO	None	DCM	rt	6	55
22	Au-Pd-rGO	None	Ethanol	rt	6	35
23	Au-Pd-rGO	None	Water	rt	6	90
24	Au-Pd-rGO	None	Neat	rt	6	50

^aReaction conditions: Indole (0.5 mmol), oxone (0.5 mmol), catalyst **1** (0.5 mol%), Catalyst **2** (2.5 μ mol%), solvent (2ml), 90 °C. ^bIsolated Yields. ^cNo reaction was observed

Table S3. Effects of catalyst and oxidant loadings on the synthesis of 2,2-Bis(indol-3-yl)indoline-3-ones

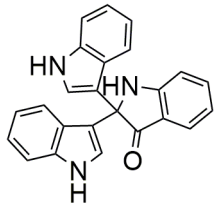


Entry	w	X	y ^c	Z	Yield (%) ^b
1	0.5	1	1	0	79
2	0.5	1	2.5	0	78
3	0.5	1	5	0	79
4	0.5	0.5	2.5	0	82
5	0.5	0.1	2.5	0	57
6	0.5	0.3	2.5	0	78
7	0.25	0.3	2.5	0	85
8	0.1	0.3	2.5	0	15
9	1	0.3	2.5	0	75
10	0.5	0	0	1	82
11	0.5	0	0	0.5	90
12	0.5	0	0	0.3	75
13	0.25	0	0	0.5	73

^aReaction conditions: Indole (0.5 mmol), H₂O (2ml), rt, 3h. ^bIsolated Yields.

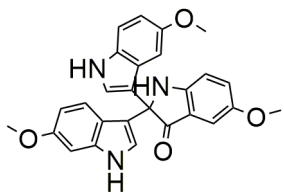
(7) Physical and Spectroscopic Data of Compounds

1H,1''H-[3,2':2',3''-terindol]-3'(1'H)-one (Table 2, entry 1)



Yellow solid; mp: 238 °C; IR (KBr) ν_{max} 3279, 2916, 1680, 1452 cm⁻¹; ¹H NMR (400 MHz, Methanol-D3) δ 7.57 – 7.54 (m, 1H), 7.48 (td, J = 7.0, 3.5 Hz, 1H), 7.34 – 7.29 (m, 4H), 7.05 (s, 2H), 7.02 (ddd, J = 8.2, 7.1, 1.1 Hz, 2H), 6.94 – 6.91 (m, 1H), 6.82 (td, J = 7.0, 3.5 Hz, 2H), 6.75 (td, J = 7.0, 3.5 Hz, 1H); ¹³C NMR (100 MHz, Methanol-D3) δ 203.87, 161.50, 137.85, 137.46, 125.88, 124.52, 124.04, 121.15, 120.40, 118.45, 117.57, 113.92, 112.00, 111.14, 68.56.

5,5',5''-trimethoxy-1H,1''H-[3,2':2',3''-terindol]-3'(1'H)-one (Table 2, entry 2)



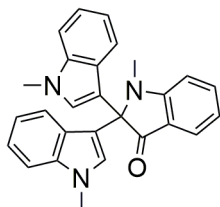
Yellow solid; mp: 214 °C; IR (KBr) ν_{max} 3440, 2257, 1626, 1465, 1022 cm⁻¹; ¹H NMR (400 MHz, Chloroform-D) δ 7.96 (s, 2H), 7.24 – 7.08 (m, 6H), 6.88 (dd, J = 16.6, 5.9 Hz, 2H), 6.81 (dd, J = 8.8, 2.6 Hz, 1H), 5.20 (s, 1H), 4.99 (s, 2H), 3.79 (s, 3H), 3.62 (s, 6H); ¹³C NMR (100 MHz, Chloroform-D) δ 154.49, 132.67, 126.60, 125.37, 115.28, 112.85, 112.64, 102.93, 69.70, 58.83, 56.20; HRMS (ESI) m/z : calcd. for C₂₄H₁₈N₃ONa [M+H]⁺ 476.1586, found 476.1578.

5,5',5''-tribromo-1H,1''H-[3,2':2',3''-terindol]-3'(1'H)-one (Table 2, entry 3)



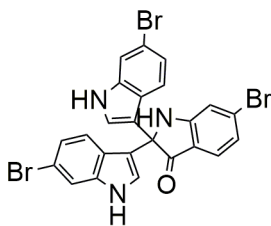
Yellow solid; mp: 248 °C; IR (KBr) ν_{max} 3440, 2257, 1626, 1465, 1035 cm⁻¹; ¹H NMR (400 MHz, Acetone-D6) δ 10.53 (s, 1H), 7.71 – 7.60 (m, 4H), 7.56 (d, J = 1.9 Hz, 2H), 7.40 (s, 1H), 7.38 (s, 2H), 7.37 (s, 1H), 7.18 (dd, J = 8.7, 1.9 Hz, 2H), 7.04 (d, J = 8.7 Hz, 1H); ¹³C NMR (100 MHz, Acetone-D6) δ 199.22, 159.74, 140.30, 136.72, 136.57, 128.12, 127.43, 125.92, 124.74, 123.38, 120.76, 114.79, 114.44, 113.97, 112.37, 109.78, 68.75.

1,1',1''-trimethyl-1H,1''H-[3,2':2',3''-terindol]-3'(1'H)-one (Table 2, entry 4)



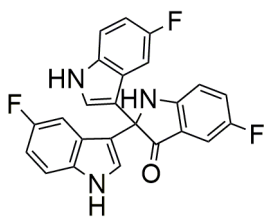
Yellow solid; mp: 228 °C; IR (KBr) ν_{max} 3453, 2929, 1653, 1452, 1022 cm⁻¹; ¹H NMR (400 MHz, DMSO-D6) δ 7.62 – 7.58 (m, 1H), 7.47 – 7.45 (m, 1H), 7.42 (dd, *J* = 8.7, 0.7 Hz, 2H), 7.19 (s, 2H), 7.13 (t, *J* = 7.4 Hz, 4H), 7.02 (d, *J* = 8.4 Hz, 1H), 6.90 – 6.86 (m, 2H), 6.74 (t, *J* = 7.4 Hz, 1H), 3.75 (s, 6H), 2.85 (s, 3H); ¹³C NMR (100 MHz, DMSO-D6) δ 200.19, 159.86, 137.78, 130.55, 127.42, 126.07, 121.74, 121.27, 119.30, 118.07, 117.06, 110.53, 87.13, 72.64, 32.96, 29.24.

6,6',6''-tribromo-1H,1''H-[3,2':2',3''-terindol]-3'(1'H)-one (Table 2, entry 5)



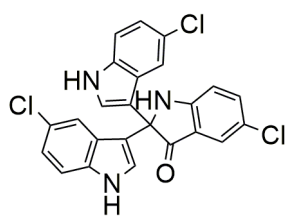
White solid; mp: 248 °C; IR (KBr) ν_{max} 3426, 2902, 1707, 1358, 1210 cm⁻¹; ¹H NMR (400 MHz, Acetone-D6) δ 10.47 (s, 2H), 7.61 (d, *J* = 1.8 Hz, 2H), 7.55 – 7.46 (m, 2H), 7.32 (s, 1H), 7.31 (s, 2H), 7.30 (s, 1H), 7.23 (d, *J* = 1.6 Hz, 1H), 7.00 (dd, *J* = 8.6, 1.7 Hz, 2H), 6.96 (dd, *J* = 8.1, 1.5 Hz, 1H). ¹³C NMR (100 MHz, Acetone-D6) δ 199.39, 161.31, 138.82, 132.34, 126.72, 125.36, 122.72, 122.35, 121.62, 118.19, 115.15, 115.10, 114.90, 114.85, 68.54.

5,5',5''-trifluoro-1H,1''H-[3,2':2',3''-terindol]-3'(1'H)-one (Table 2, entry 6)



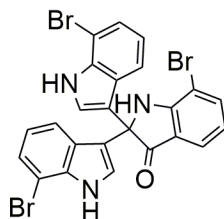
Yellow solid; mp: 101.4 °C; IR (KBr) ν_{max} 3453, 2916, 1720, 1371, 1210 cm⁻¹; ¹H NMR (400 MHz, Methanol-D3) δ 7.27 (td, *J* = 8.9, 2.7 Hz, 1H), 7.21 (dd, *J* = 8.9, 4.5 Hz, 2H), 7.16 (dd, *J* = 7.5, 2.7 Hz, 1H), 7.08 (s, 2H), 6.90 (dd, *J* = 8.9, 3.9 Hz, 1H), 6.85 (dd, *J* = 10.3, 2.5 Hz, 2H), 6.73 (td, *J* = 9.1, 2.5 Hz, 2H). ¹³C NMR (100 MHz, Acetone-D6) δ 201.85, 160.00, 159.34, 157.70, 135.79, 127.98, 127.57, 116.36, 111.51, 111.25, 107.02, 106.44, 70.54.

5,5',5''-trichloro-1H,1''H-[3,2':2',3''-terindol]-3'(1'H)-one (Table 2, entry 7)



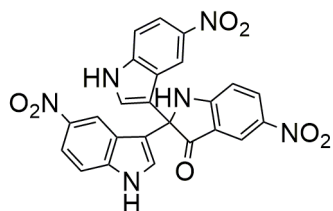
Yellow solid; mp: 199 °C; IR (KBr) ν_{max} 3453, 2916, 1734, 1356, 1210 cm⁻¹; ¹H NMR (400 MHz, Methanol-D3) δ 7.46 (d, J = 2.2 Hz, 1H), 7.42 (dd, J = 8.7, 2.2 Hz, 1H), 7.23 (t, J = 7.3 Hz, 3H), 7.21 (d, J = 2.0 Hz, 2H), 7.09 (s, 2H), 6.95 (dd, J = 8.6, 2.0 Hz, 2H), 6.91 (d, J = 8.7 Hz, 1H). ¹³C NMR (100 MHz, Acetone-D6) δ 199.22, 159.74, 140.30, 136.72, 136.57, 128.12, 127.43, 125.92, 124.74, 123.38, 120.76, 114.79, 114.44, 113.97, 112.37, 109.78, 68.75.

7,7',7''-tribromo-1H,1''H-[3,2':2',3''-terindol]-3'(1'H)-one (Table 2, entry 9)



Yellow solid; mp: 117.5 °C; ¹H NMR (400 MHz, Methanol-D3) δ 7.68 (dd, J = 7.7, 1.1 Hz, 1H), 7.50 (dd, J = 7.7, 1.1 Hz, 1H), 7.24 (dd, J = 8.1, 0.9 Hz, 2H), 7.18 (ddd, J = 7.6, 2.3, 0.8 Hz, 3H), 7.14 (s, 2H), 7.10 – 7.05 (m, 1H), 6.74 (d, J = 7.9 Hz, 2H), 6.71 – 6.63 (m, 2H). ¹³C NMR (100 MHz, Methanol-D3) δ 203.27, 159.59, 137.20, 128.49, 126.89, 121.44, 120.65, 120.40, 116.02, 106.41, 105.73, 70.29.

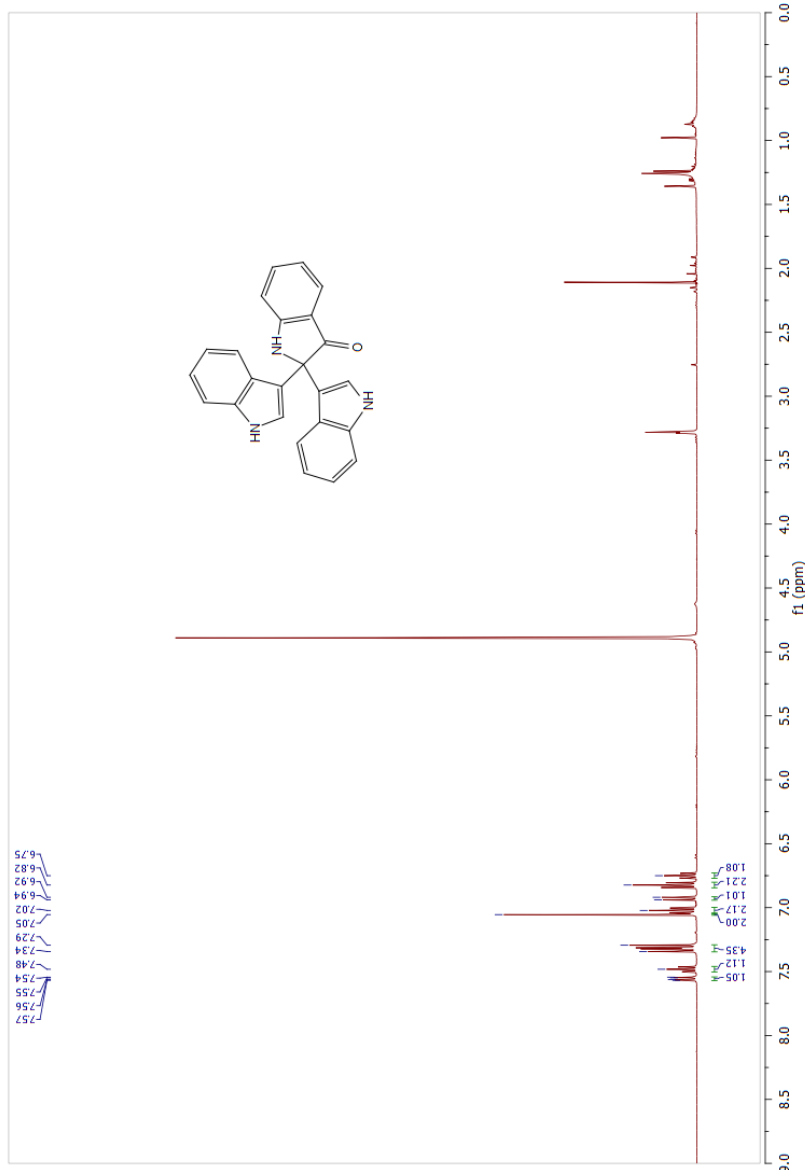
5,5',5''-trinitro-1H,1''H-[3,2':2',3''-terindol]-3'(1'H)-one (Table 2, entry 8)

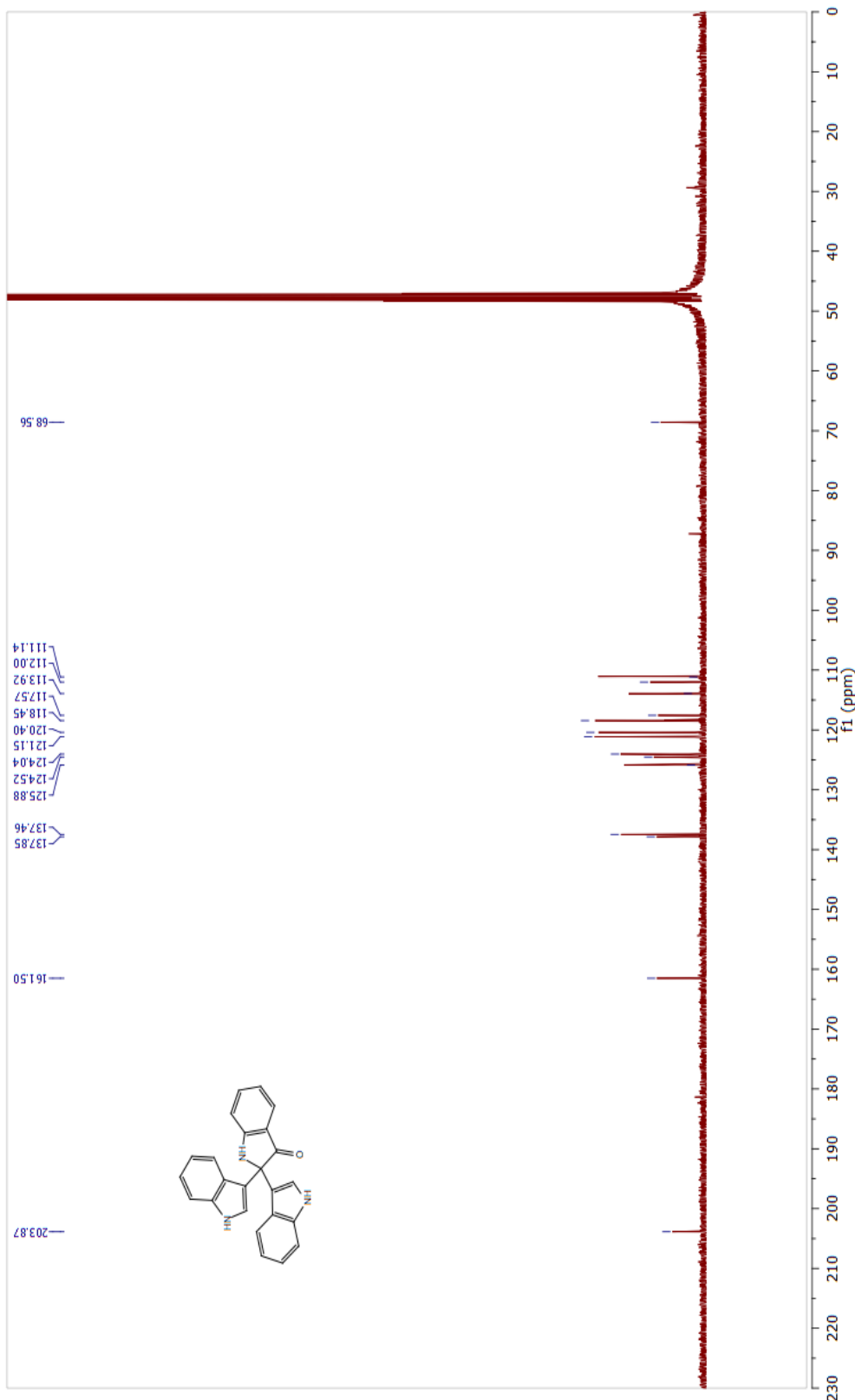


Yellow solid; mp: 216 °C; IR (KBr) ν_{max} 3440, 2997, 1761, 1371, 1237, 1063 cm⁻¹; ¹H NMR (400 MHz, Acetone-D6) δ 11.17 (s, 1H), 9.02 (s, 1H), 8.77 (d, J = 2.7 Hz, 1H), 8.52 (dd, J = 8.6, 2.6 Hz, 1H), 8.48 – 8.43 (m, 1H), 8.37 (d, J = 2.1 Hz, 1H), 8.34 – 8.28 (m, 1H), 8.23 (dd, J = 9.0, 1.9 Hz, 1H), 8.16 – 8.07 (m, 1H), 8.02 – 7.97 (m, 1H), 7.75 (d, J = 2.3 Hz, 1H), 7.64 (d, J = 9.0 Hz, 1H), 7.30 – 7.11 (m, 1H), 6.98 (dd, J = 16.8, 9.1 Hz, 1H).

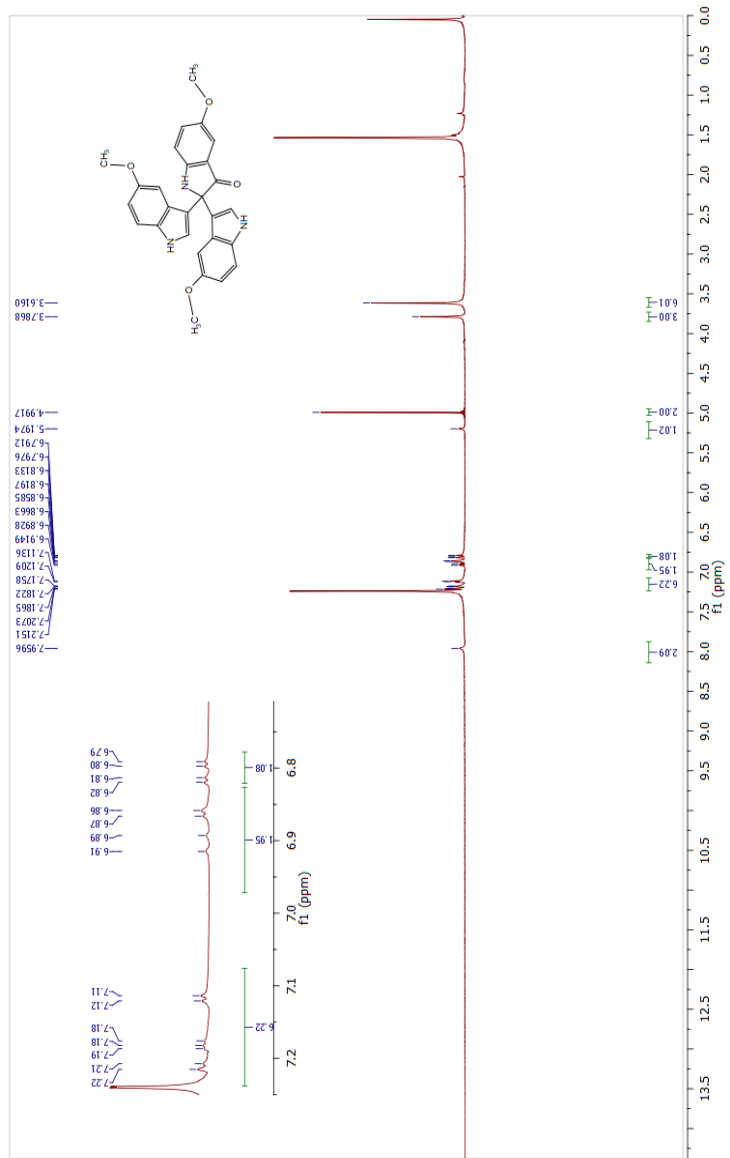
(8) ^1H NMR and ^{13}C NMR spectra of compounds

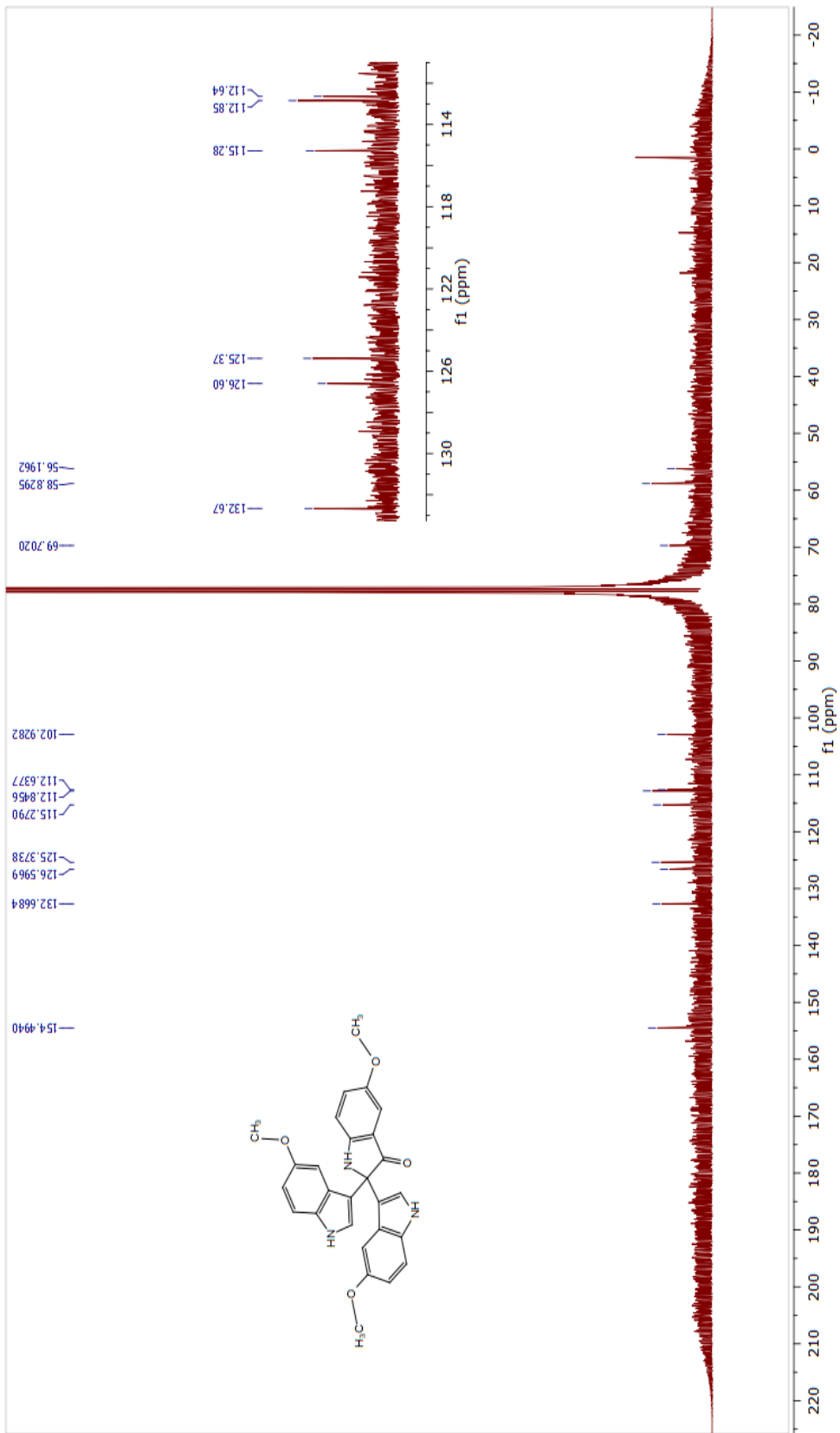
1H,1''H-[3,2':2',3''-terindol]-3'(1'H)-one (Table 2, entry 1)



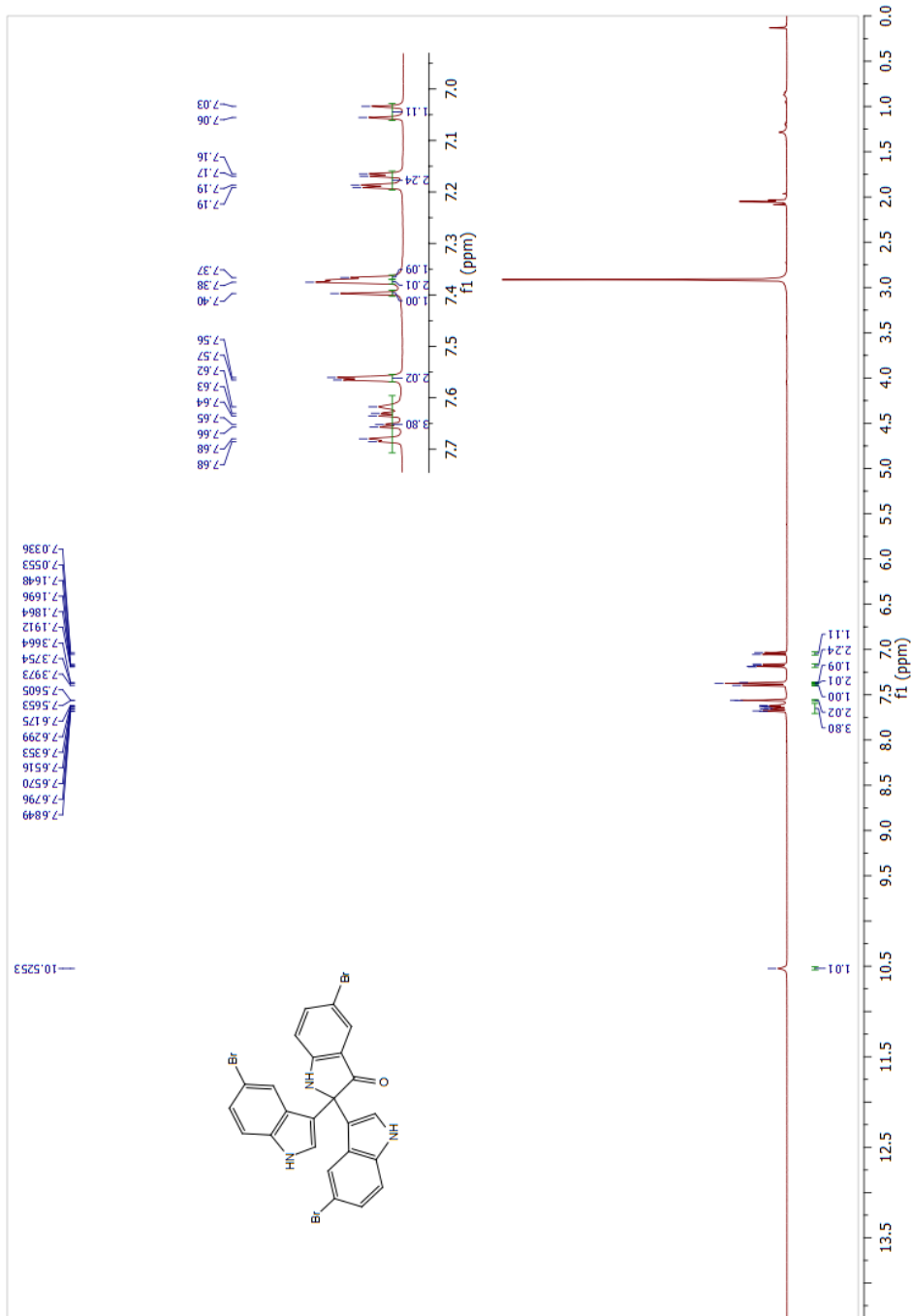


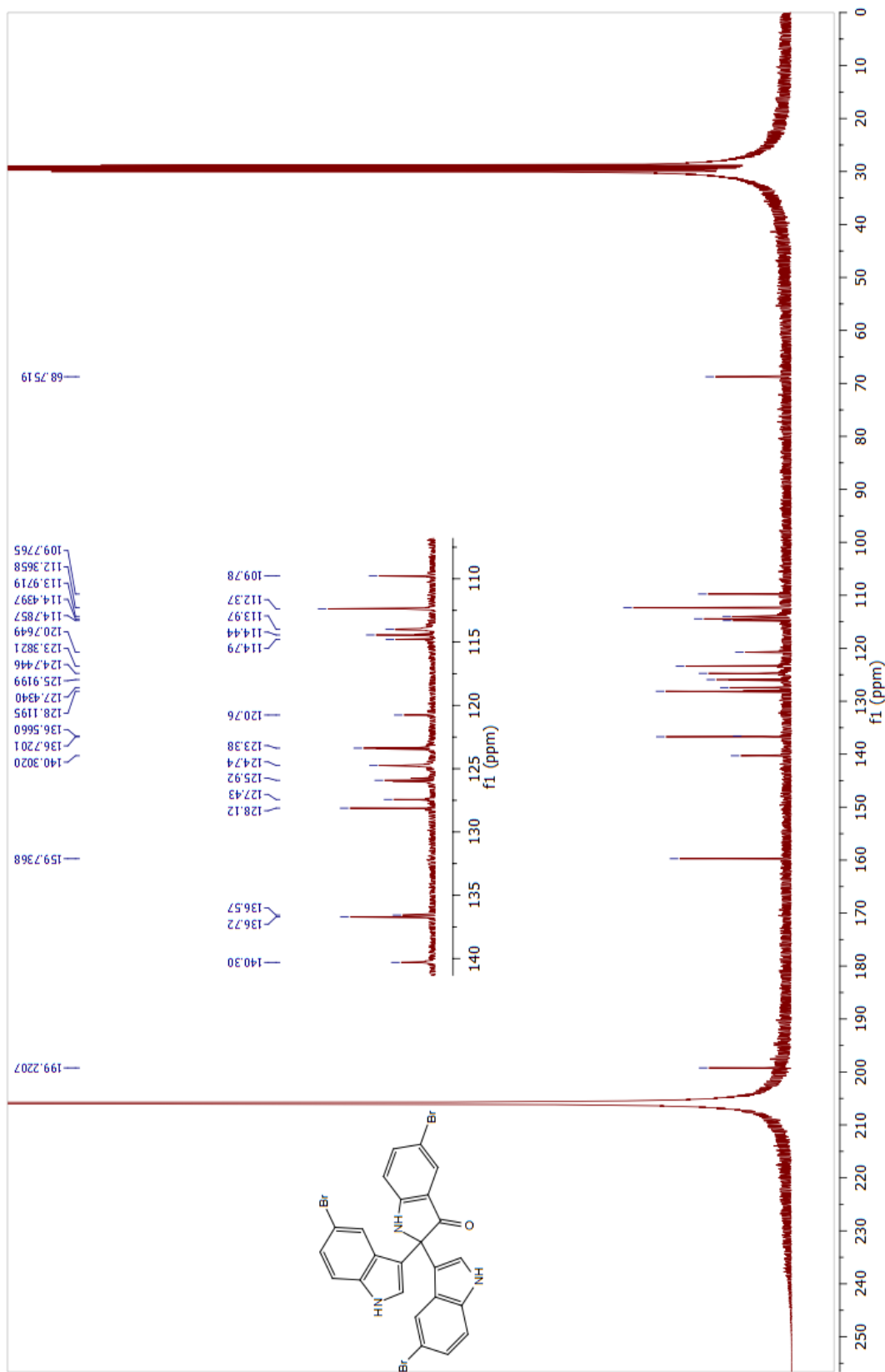
5,5',5''-trimethoxy-1H,1''H-[3,2':2',3''-terindol]-3'(1'H)-one (Table 2, entry 2)



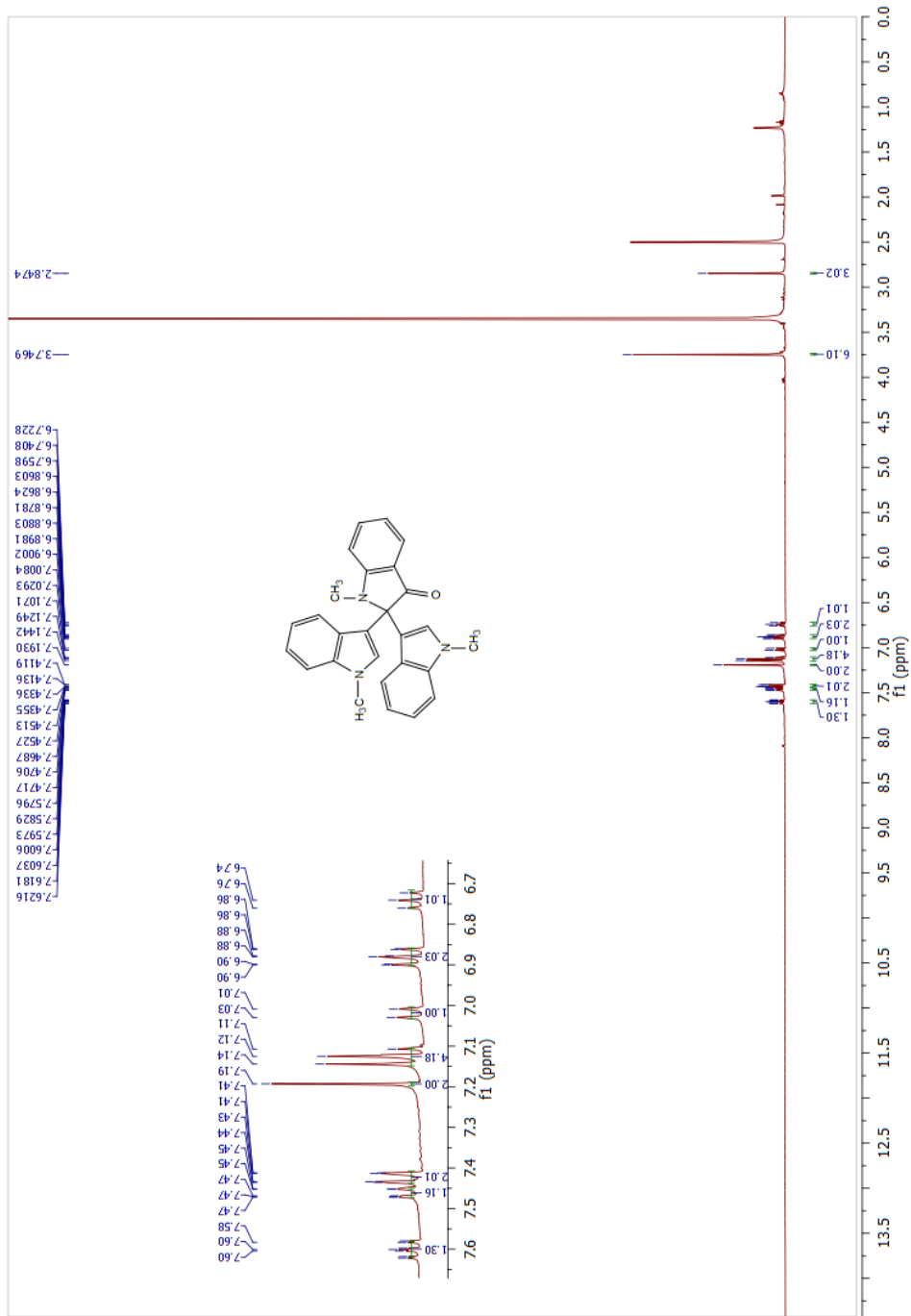


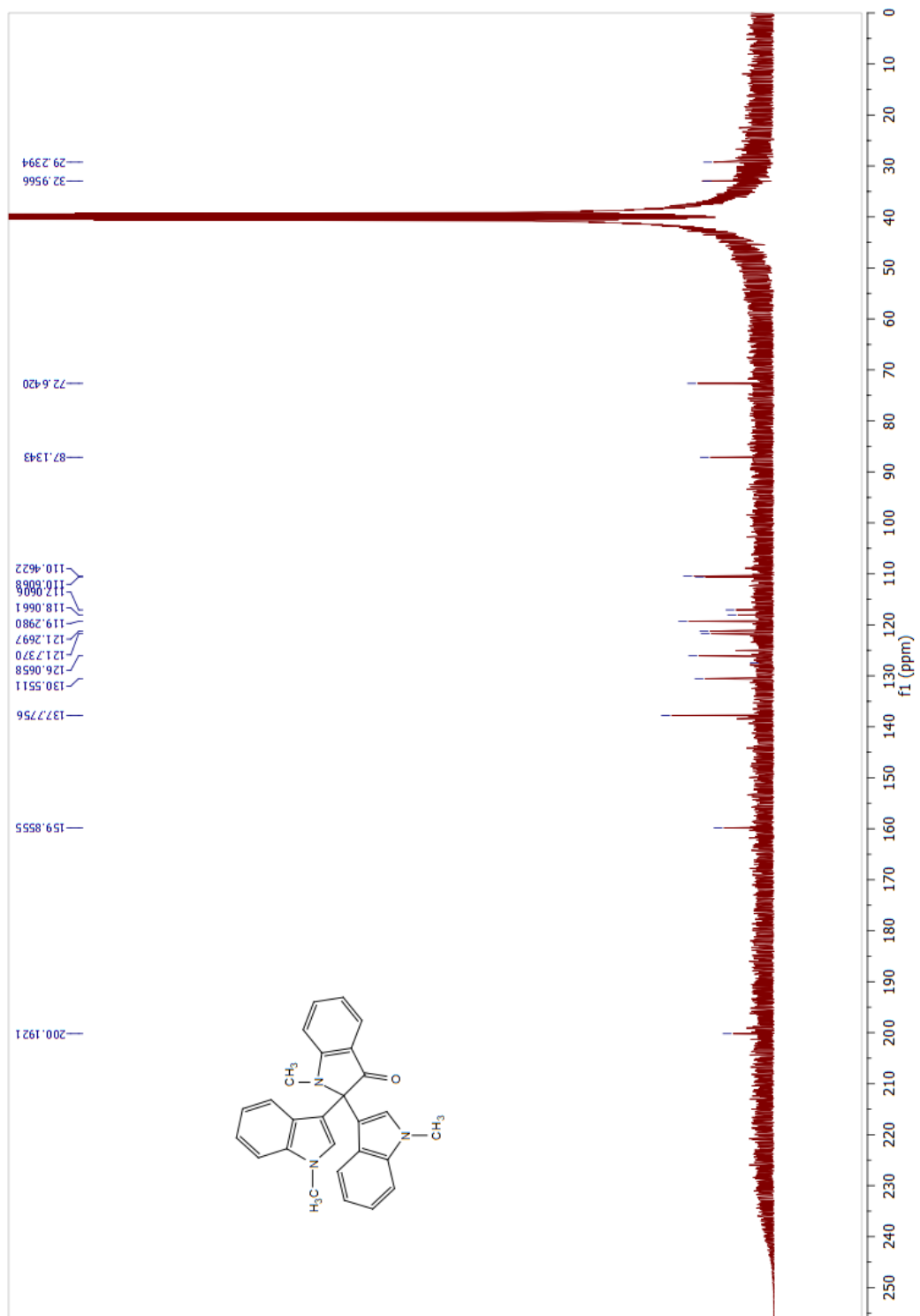
5,5',5''-tribromo-1H,1''H-[3,2':2',3''-terindol]-3'(1'H)-one (Table 2, entry 3)



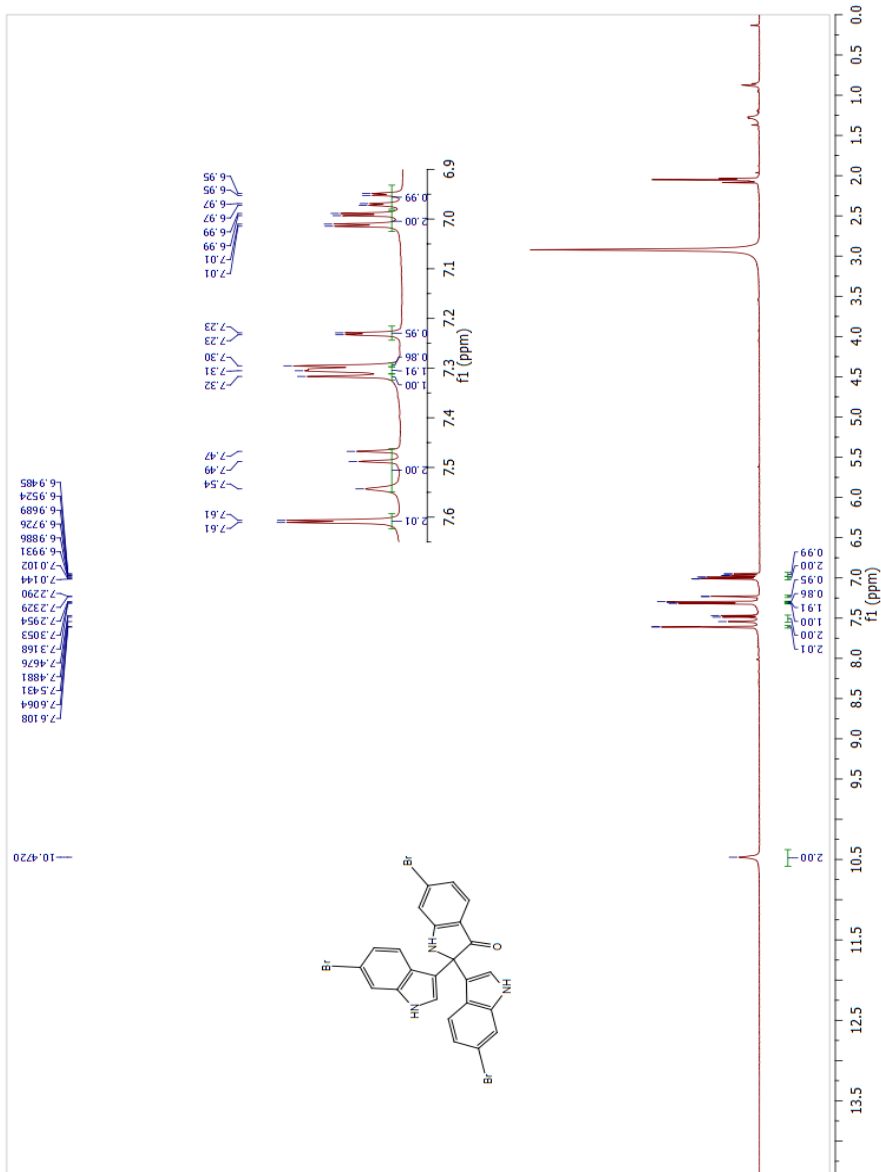


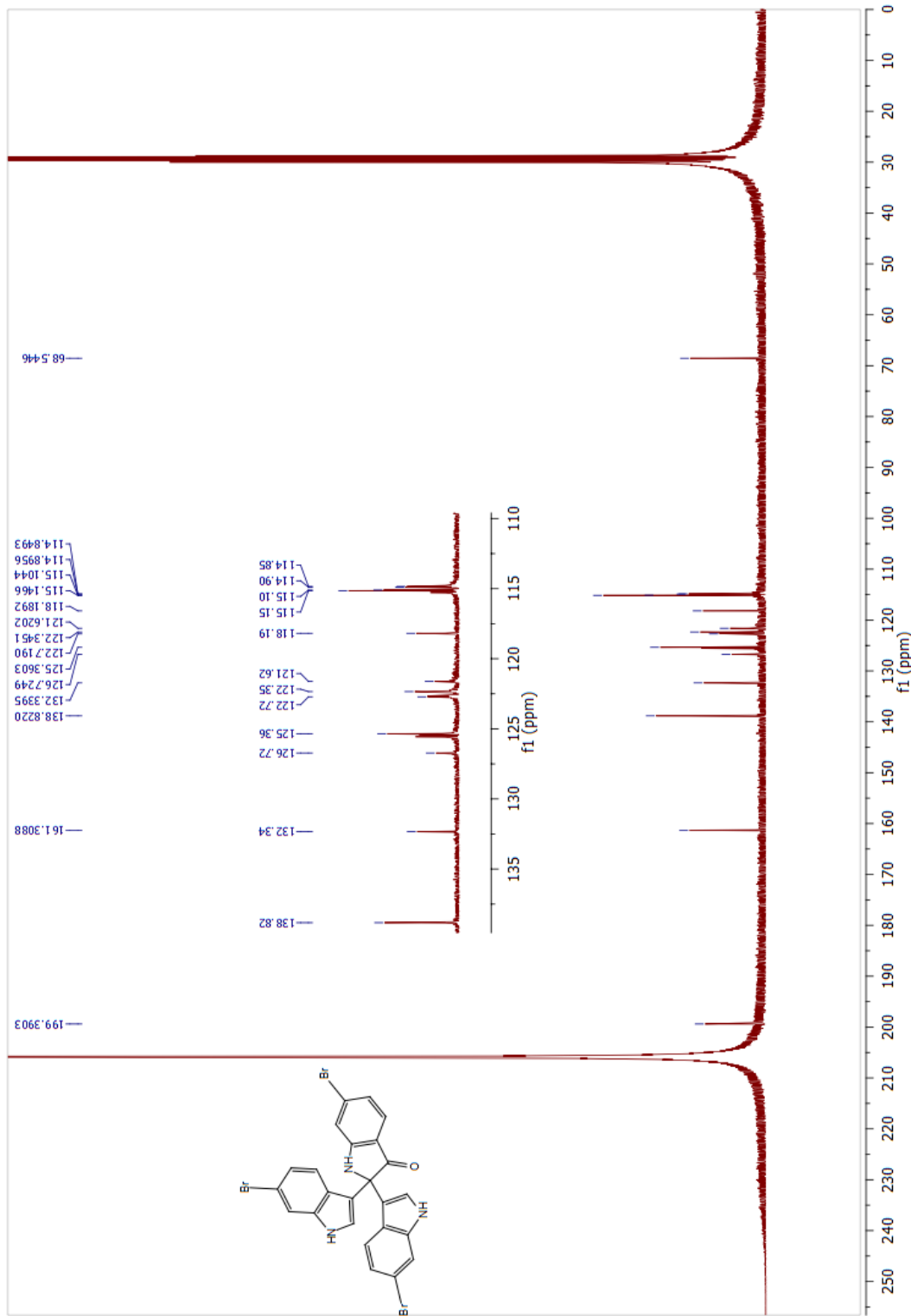
1,1',1''-trimethyl-1H,1''H-[3,2':2',3''-terindol]-3'(1'H)-one (Table 2, entry 4)



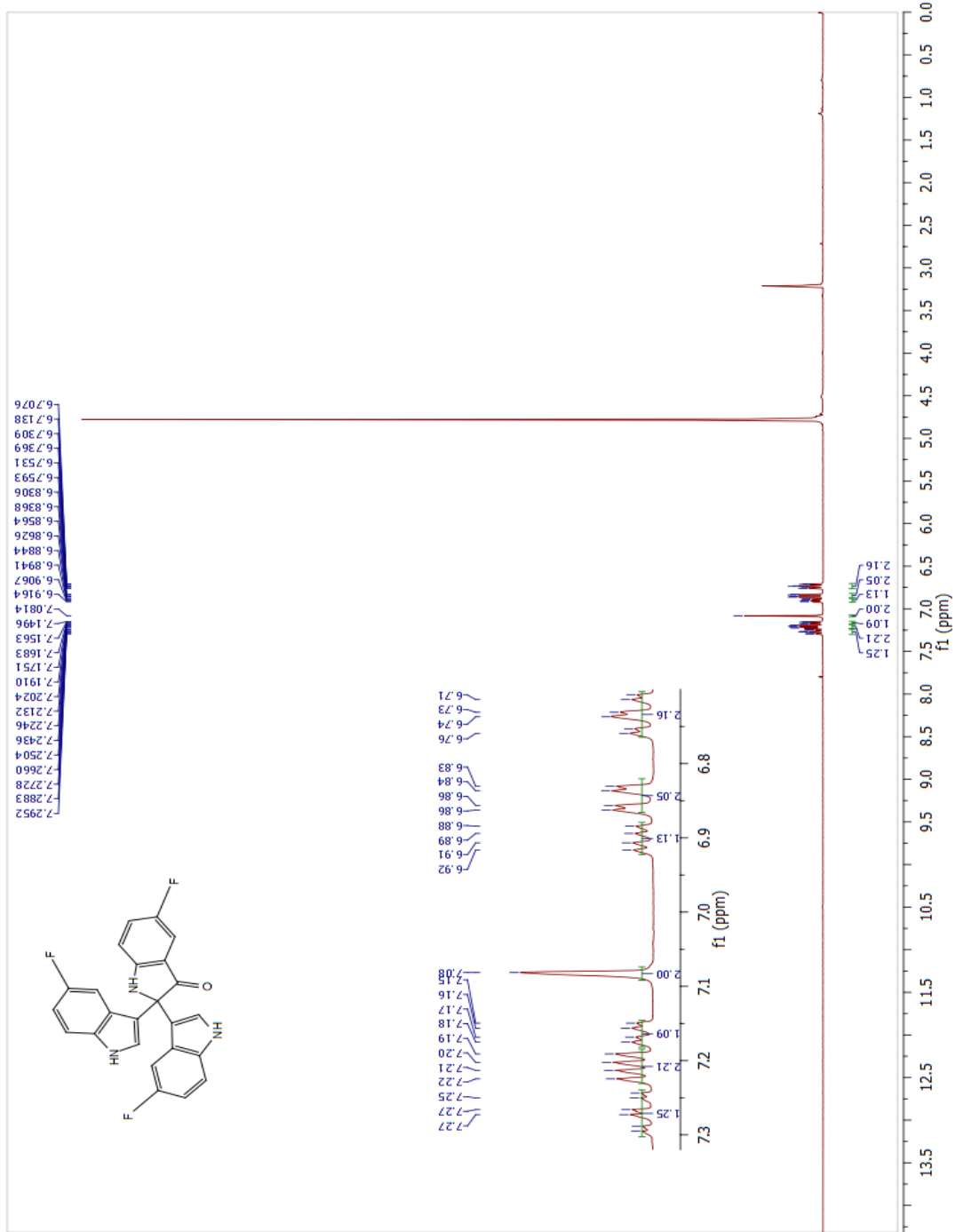


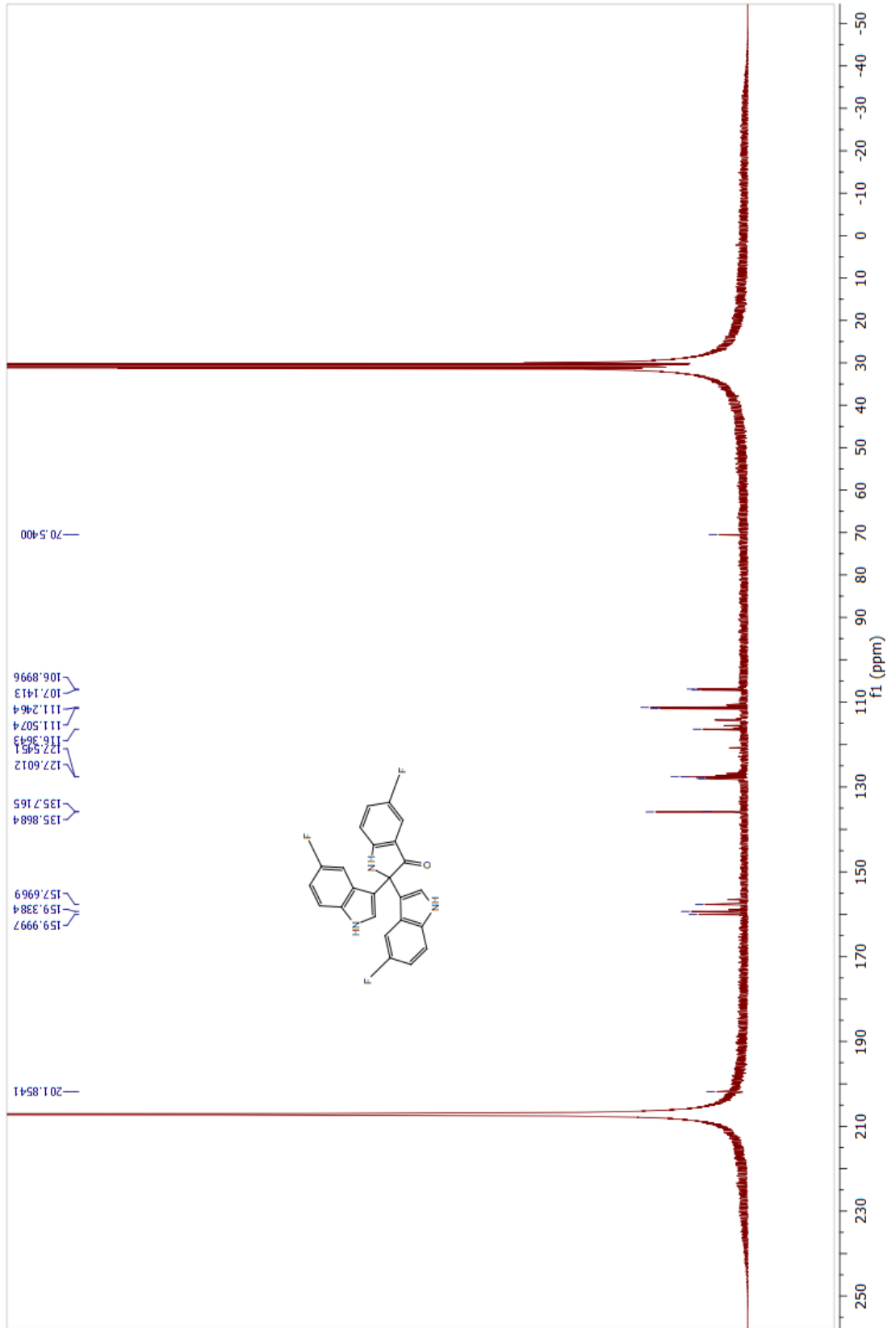
6,6'',6'''-tribromo-1H,1''H-[3,2':2',3''-terindol]-3'(1'H)-one(Table 2, entry 5)



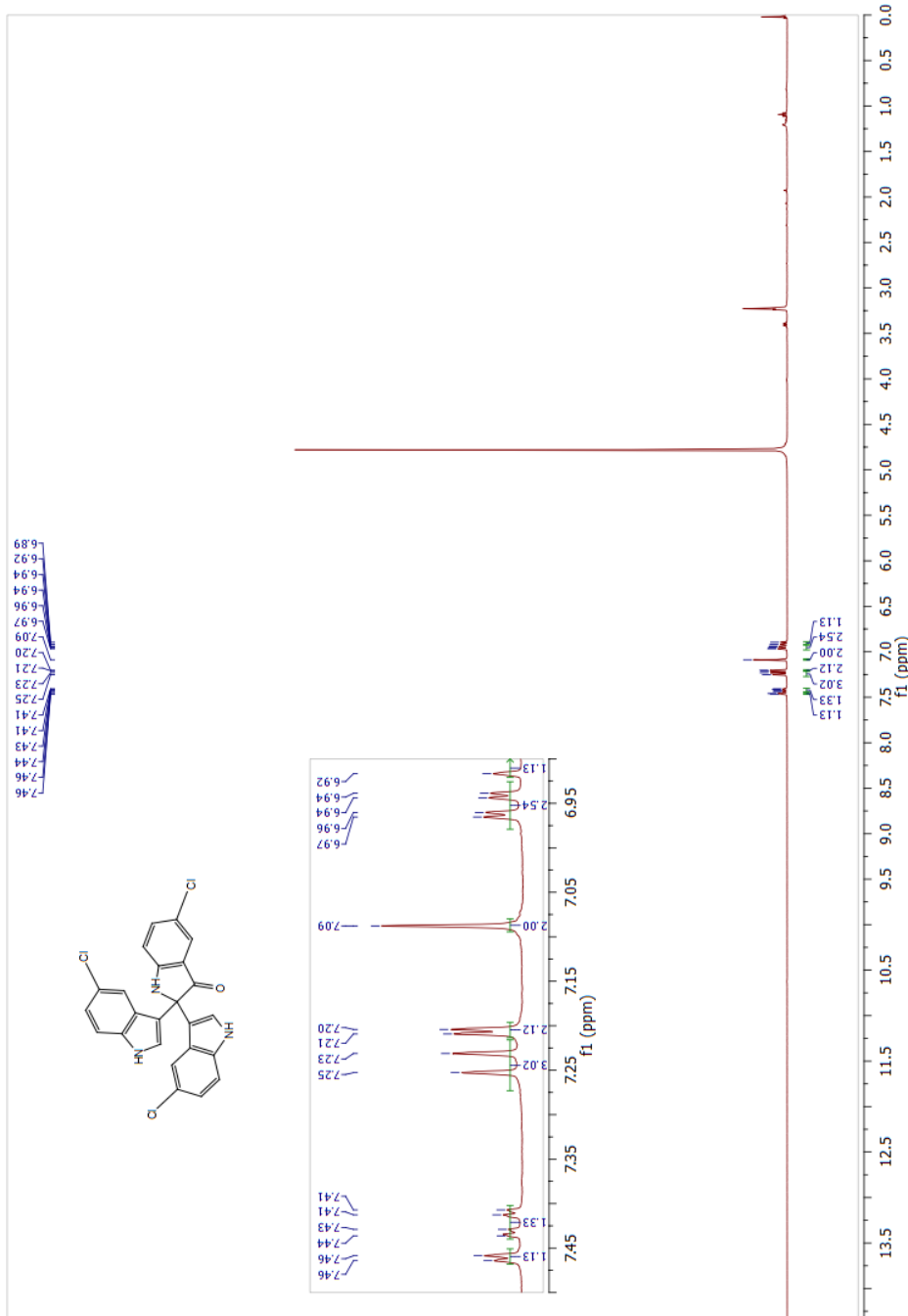


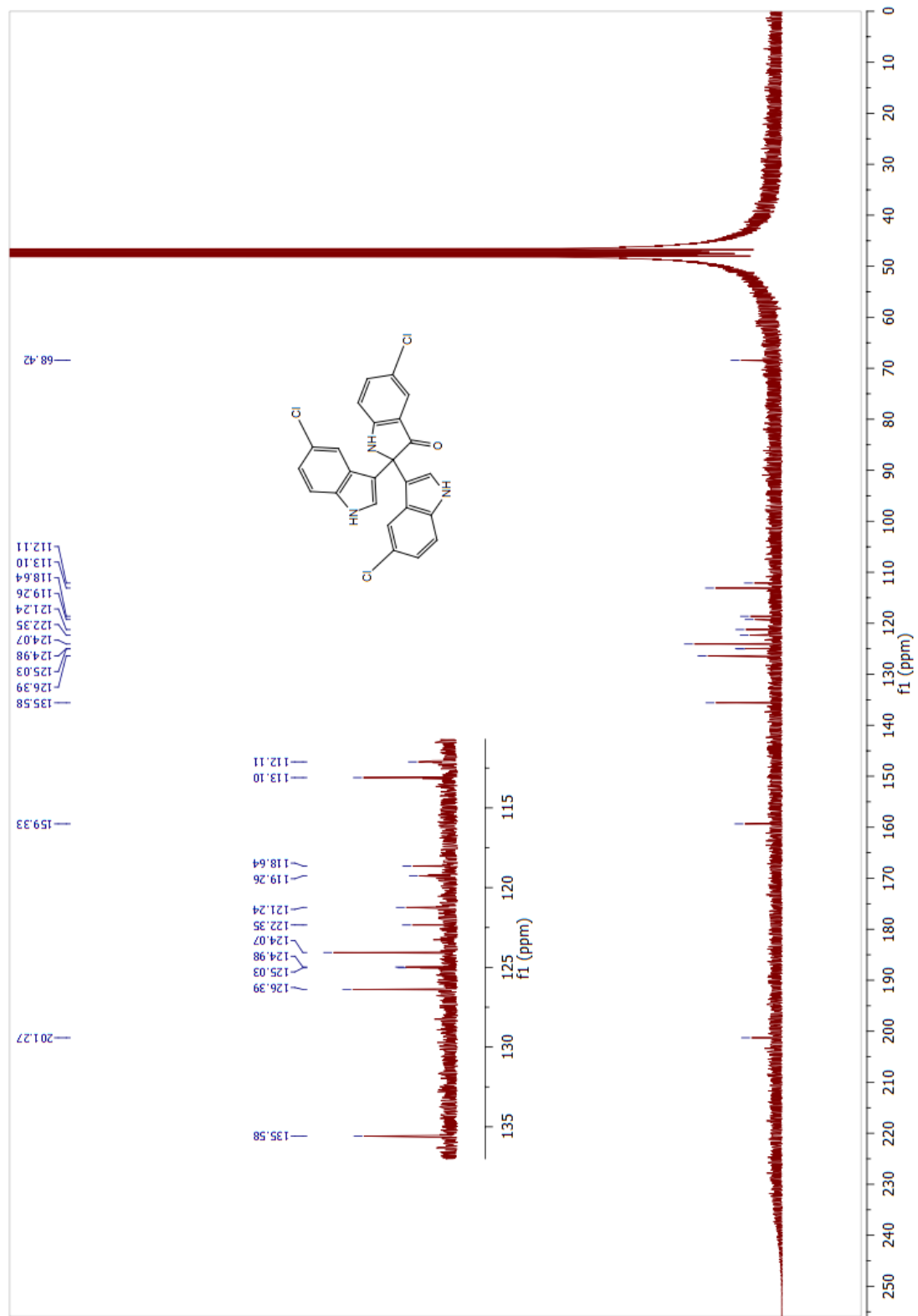
5,5',5''-trifluoro-1H,1''H-[3,2':2',3''-terindol]-3'(1'H)-one (Table 2, entry 6)



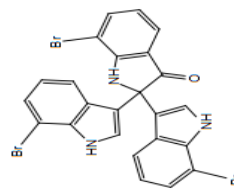
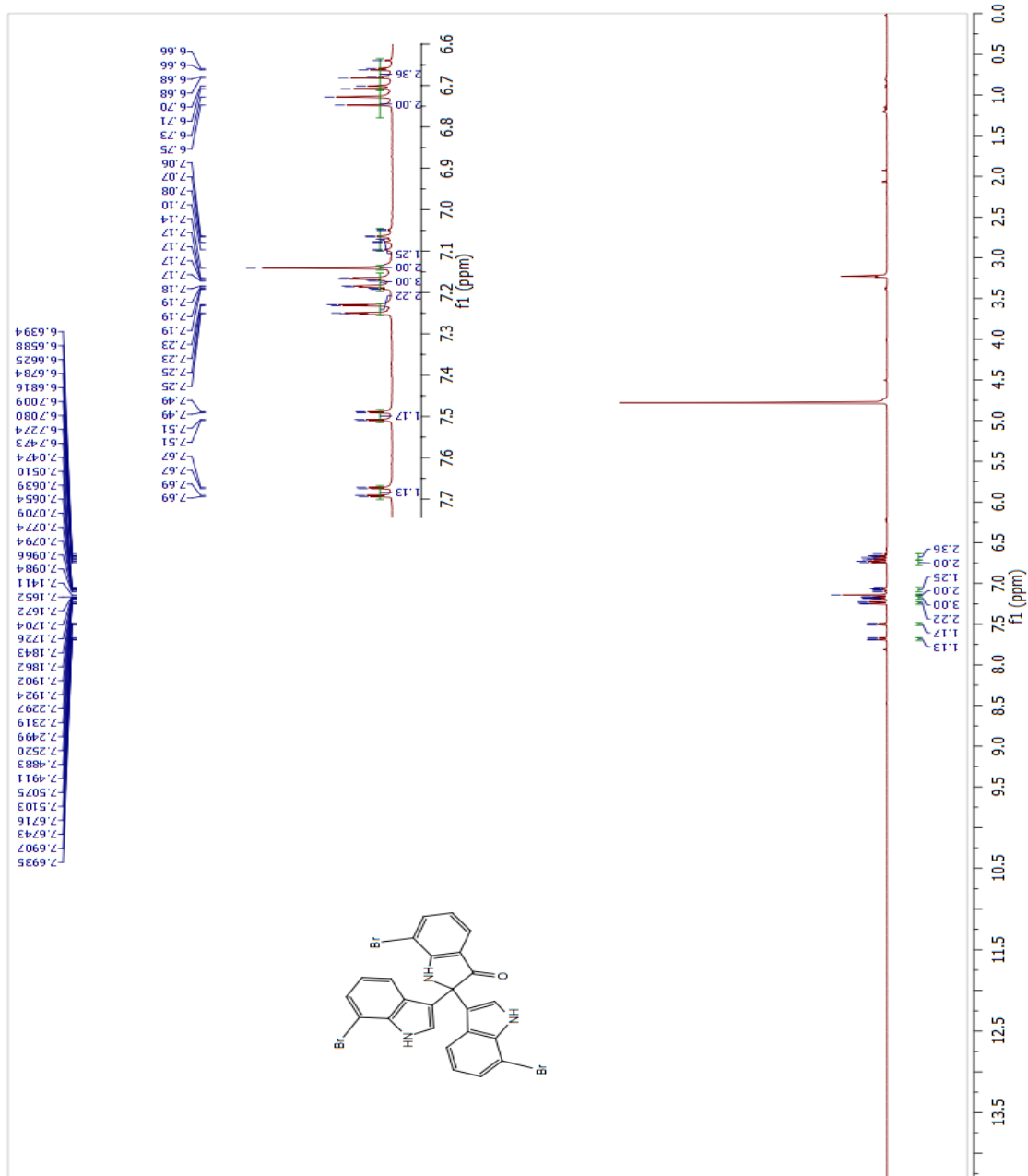


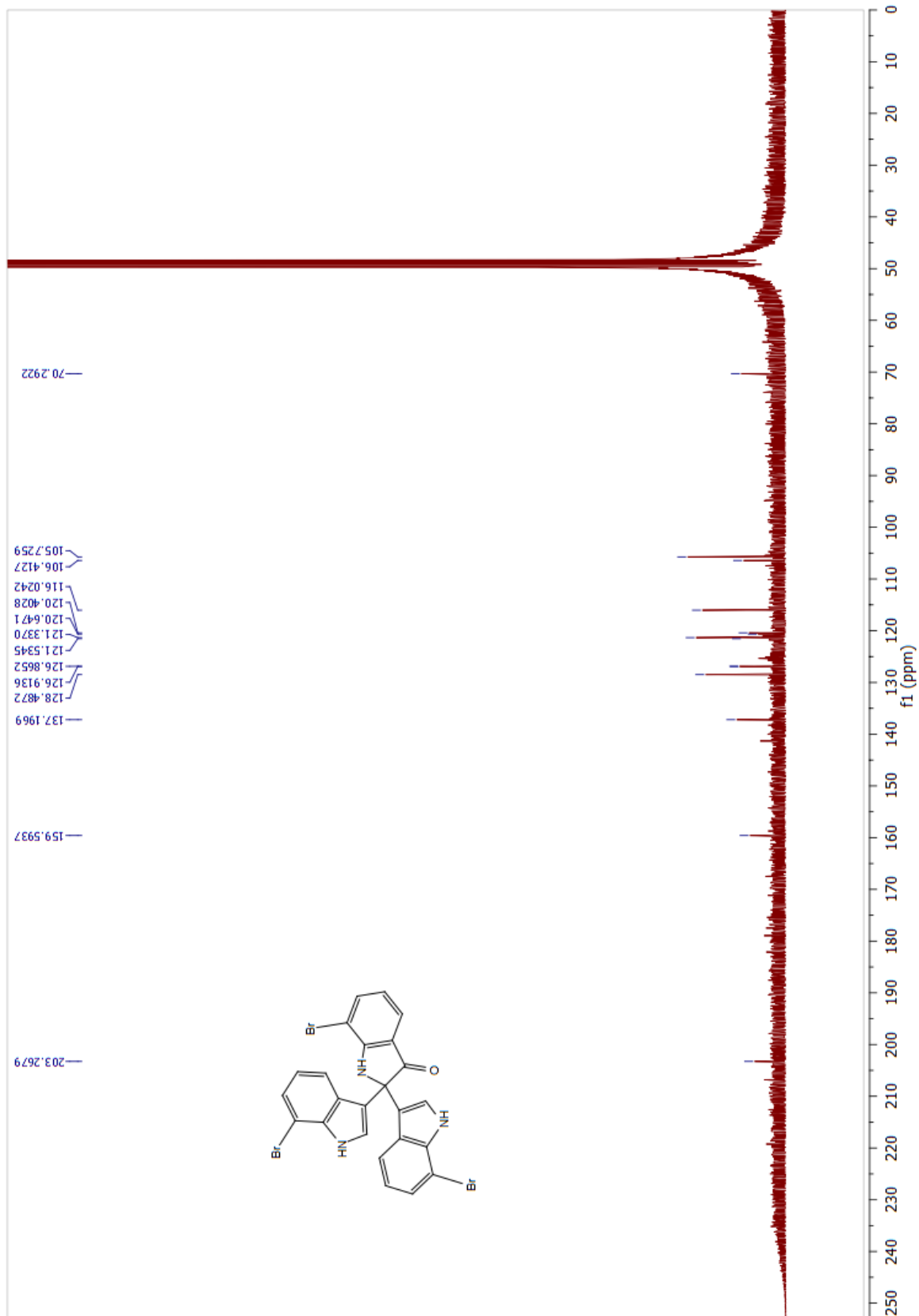
5,5',5''-trichloro-1H,1'H-[3,2':2',3''-terindol]-3'(1'H)-one (Table 2, entry 7)



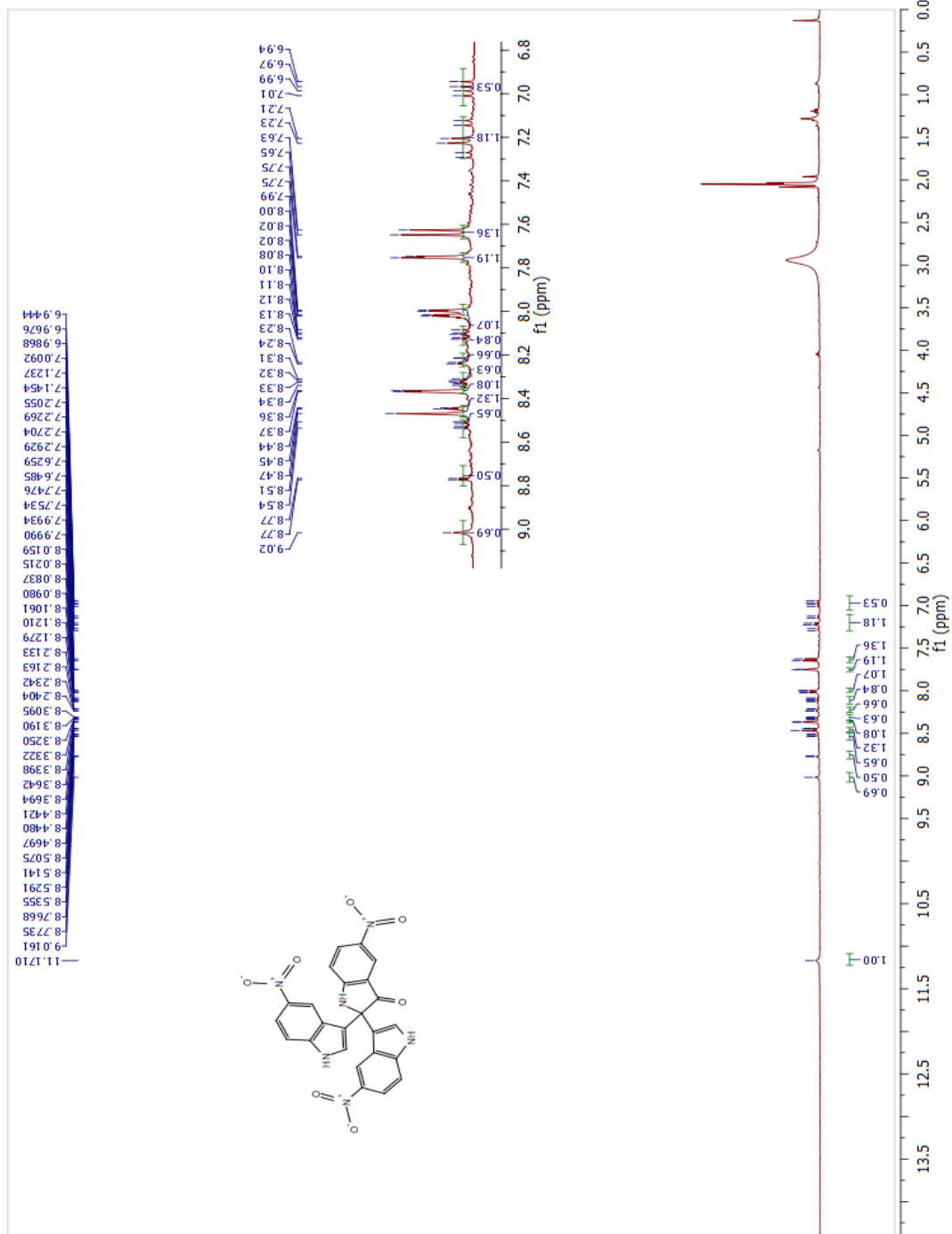


7,7',7''-tribromo-1H,1''H-[3,2':2',3''-terindol]-3'(1'H)-one (Table 2, entry 8)





5,5',5''-trinitro-1H,1''H-[3,2':2',3''-terindol]-3'(1'H)-one (Table 2, entry 9)



(9)Table S4. List of selected previous works

Sl. No.	Starting material	Conditions	(%) Yield	Product	Advantage of our work	Reference
1	<i>N</i> -methyl isatin, Phenylacetylene, Phenyl isocyanate	DBU (0.31 mmol, 0.5 equiv) and CuI (10 mol %), in anhydrous toluene (3 mL) rt, 12 h under N ₂ atmosphere	64-86	(Z)-4'-benzylidene-1-methyl-3'-phenylspiro[indoline-3,5'-oxazolidine]-2,2'-dione	Simpler starting material	4
2	Oxoindolines, 1,3-diketones (1:1)	SFAA catalyst (5 mol%), 0 °C, 48 h (SFAA = hybrid-type squaramide-fused amino alcohol organocatalyst)	82-98	Spiro-conjugated 2-aminopyrans		5
3	<i>N</i> -Methyl spiro-epoxy oxindole, indole (1:3)	CH ₃ COOH, H ₂ O, 80 °C, 6h	52-66	3, 3'-bisindoles		6
4	Indole	Laccase, O ₂ , 2 bar, 48 h			Mild reaction conditions	7
5	Indole	Benzoic acid (0.5 mmol), TEMPO (0.7 mmol), CH ₃ CN (0.6 mL), 65 °C, 3 days	70-93	2-(1 <i>H</i> -indol-3-yl)-2,3'-biindolin-3-ones		8
6	Indole	Benzoic acid (0.1 mmol), TEMPO (0.35 mmol), pyridine (1 mL), 65 °C, 48 h	56-90	C3-C3' bisindolin-2-ones		9
7	Indole	PdCl ₂ (5 mol %), TBHP (70% aq, 2.2 equiv), MnO ₂ (2 equiv), MeCN (1 mL), 60 °C, 5 h	80-90	Indoline-3-ones		10
8	2-arylindoles	i) Methylene blue /hv/O ₂ / MeOH ii) HAr/AcOH	77-93	2,2-diaryl-1,2-dihydro-3 <i>H</i> -indol-3-ones		11
9	2-arylindoles	20 mol% Cu(OH) ₂ ·CuCO ₃ (0.06 mmol), DMSO (2 mL), O ₂ (1 atm), 130 °C, 48 h.	16-90	15a-phenyl-5 <i>H</i> -diindolo[1,2-a:3',2'-c]quinolin-15(15a <i>H</i>)-one		12
10	2-phenylindole, indole (1:2)	TBHP (6.0 equiv., 70% aq.), HFIP (1.0 ml), 90 °C, 150 W, 30 min	20-94	2,2-disubstituted indolin-3-ones	Simpler starting material, Mild reaction conditions	13
11	<i>N</i> -substituted Indole	NaNO ₂ (0.5 mmol), CH ₃ SO ₃ H (1.0 mmol), pyridine (0.6 mL), rt, overnight	51-91	2-(1 <i>H</i> -indol-3-yl)-2,30-biindolin-3-one		14
12	Benzylxyallene, oxindole	2.5 mol% Pd ₂ (dba) ₃ ·CHCl ₃ , 5.5 mol% (R,R)-Ligand, 10 mol% acid, THF, rt, 4h	81-87	Phenylindolin-2-ones		15
13	Indole, Cyclic imine	Chiral Phosphoric acid (5 mol%), CHCl ₃ /Toluene (3:1), -70 °C, 3-12 h (Friedel-Crafts Reaction)	79-91	Indolindolinone		16
14	<i>N</i> -substituted Indole, Ethyl Glyoxylate(1:1.5)	Ti(O-i-Pr)4 (10 mol%), (S)-BINOL (20 mol%) in 1 mL of Et ₂ O, 45–72 h	62-96	3-Indolyl-(hydroxy)acetates		17
16	<i>N</i> -substituted Indole	TBHP, 100 °C, 3h	52-84	Indolinones	Mild reaction	18

17	<i>N</i> -substituted Indole	I ₂ (10 mol %), Cyclohexanone(10 mol %), TBHP (70 % in H ₂ O, 0.7 eq.), rt, 7-12 h	17-92	indolin-3-ones	conditions	19
18	Aryl azides	10 mol % of Cu(OTf) ₂ , DCM, rt, 24 h	41-93	2-Indolylindolin-3-ones	Simpler starting material	20
19	Indole, isatin (1:1)	MoS ₂ - C ₃ N ₄ , H ₂ O, rt, 12 h	78-94	[3,3':3',3"-terindolin]-2'-one		21

(10) Crystallographic data and molecular structure of compound 8c

5,5',5"-tribromo-1*H*,1"*H*-[3,2':2',3"-terindol]-3'(1'H)-one (Table 2, entry 3)

X-ray structure determination was obtained *via* slow evaporation of compound **8c** in acetone at room temperature.

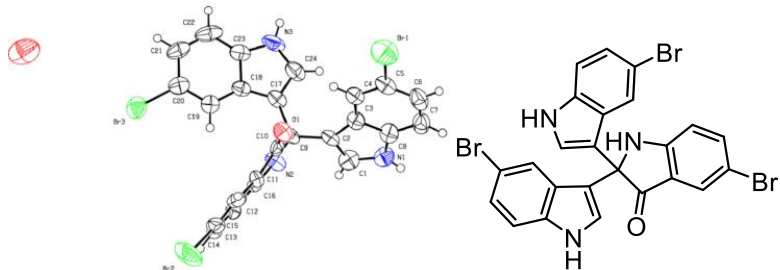
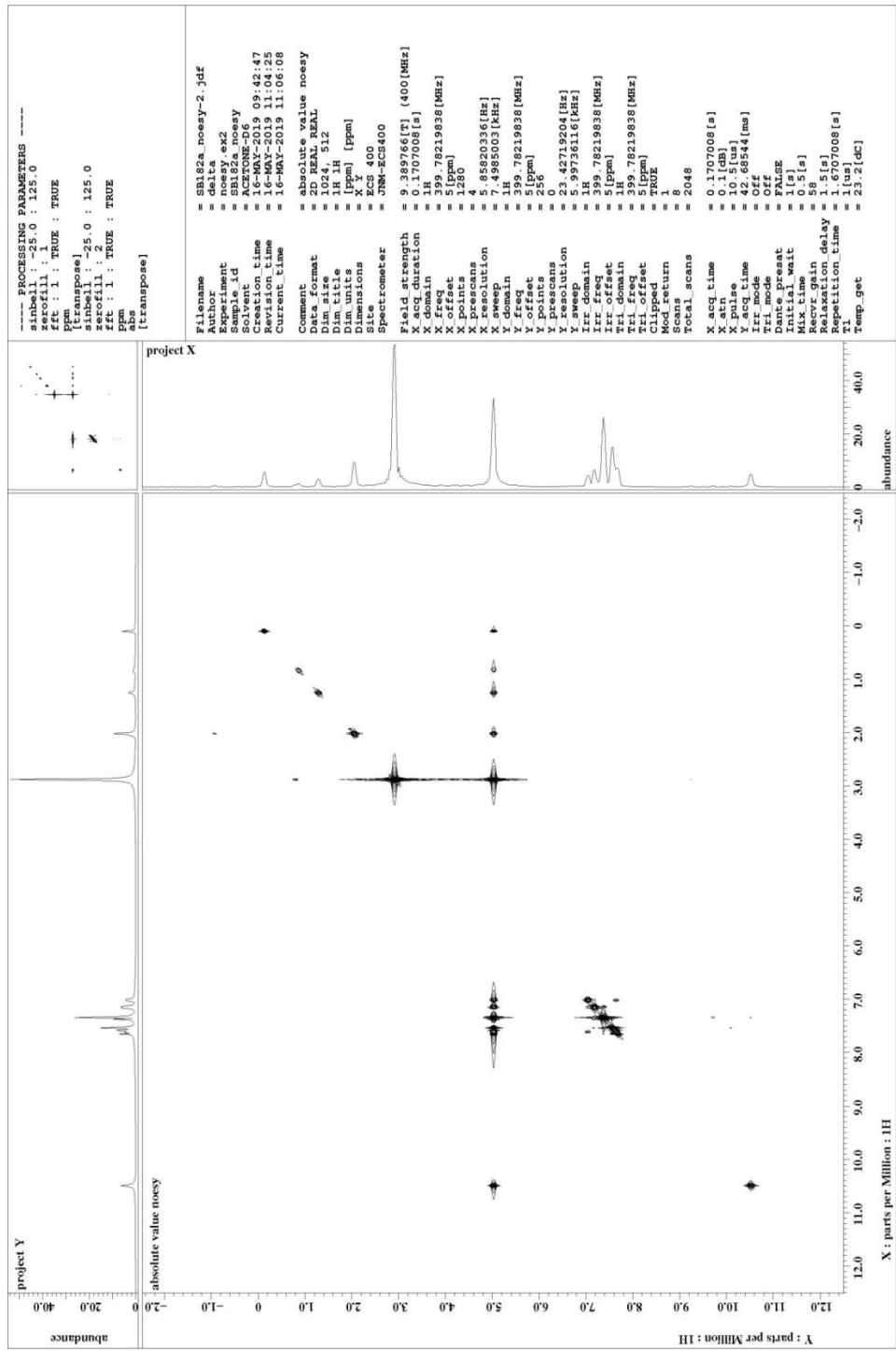


Fig. S21 X-ray crystal structure of **8c**; ellipsoids depicted at 50% probability level

Table S5. Crystal data and structure refinement for compound **8c** (CCDC: 1920668)

Empirical Formula	4 (C ₂₄ H ₁₄ Br ₃ N ₃ O),O		F(000)	1176
Formula Weight			Reflections collected	5578
Temperature	296 K		Max. and min. transmission	0.195 and 0.437
Wavelength	0.71073		Refinement method	Full-matrix-least squares on F ²
Crystal system				
Space group	P 21 21 21			
Unit cell dimensions	a = 8.6559(5) Å	α = 90°		
	b = 15.6308(9) Å	β = 90°		
	c = 16.2787(8) Å	γ = 90°		
Volume	2202.5(2) Å ³			
Z	4			
Density (calculated)	1.822 g/cm ³			

(11) NOE NMR of compound 8c



(12) References

- 1 W. S. Hummers and R. E. Offeman, *J. Am. Chem. Soc.* 1958, **80**, 1339.
- 2 A. R. Siamaki, A. E. R. S. Khder, V. Abdelsayed, M. S. E. Shall, B. F. Gupton, *J. Catal.*, 2011, **279**, 1-11.
- 3 S. Guo, L. Wang, S. Dong and E. Wang, *J. Phys. Chem. C*, 2008, **112**, 13510-13515.
- 4 G. R. Potuganti, D. R. Indukuri, J. B. Nanubolu and M. Alla, *J. Org. Chem.*, 2018, **83**, 15186-5194.
- 5 M. Chennapuram, I. A. Owolabi, C. Seki, Y. Okuyama, E. Kwon, K. Uwai, M. Tokiwa, M. Takeshita and H. Nakano, *ACS Omega*, 2018, **3**, 11718-11726.
- 6 S. Hajra, S. Maity, S. Roy, R. Maity and S. Samanta, *Eur. J. Org. Chem.*, 2019, **5**, 969-987.
- 7 C. Ganachaud, V. Garfagnoli, T. Tron, G. Iacazio, *Tetrahedron Lett.*, 2008, **49**, 2476-2478
- 8 W. Qin, Q. Chang, Y. Bao, N. Wang, Z. Chen and L. Liu, *Org. Biomol. Chem.*, 2012, **10**, 8814-8821.
- 9 F. Lin, Y. Chen, B. Wang, W. Qin and L. Liu, *RSC Adv.*, 2015, **5**, 37018-37022.
- 10 S. K. Guchhait, V. Chaudhary, V. A. Rana, G. Priyadarshani, S. Kandekar and M. Kashyap, *Org. Lett.*, 2016, **18**, 1534-1537.
- 11 L. Ke-Qing, *Synth. Commun.*, 1995, **25**, 3831-3835.
- 12 P. Sang, Y. Xie, J. Zou and Y. Zhang, *Adv. Synth. Catal.*, 2012, **354**, 1873-1878.
- 13 X. Jiang, B. Zhu, K. Lin, G. Wang, W. Su and C. Yu, *Org. Biomol. Chem.*, 2019, **17**, 2199-2203.
- 14 J. Xue, Y. Bao, W. Qin, J. Zhu, Y. Kong, H. Qu, Z. Chen and L. Liu, *Synth. Commun.*, 2014, **44**, 2215-2221.
- 15 B. M. Trost, J. Xie and J. D. Sieber, *J. Am. Chem. Soc.*, 2011, **133**, 20611-20622.
- 16 M. Rueping, S. Raja and A. Núñez, *Adv. Synth. Catal.* 2011, **353**, 563-568.
- 17 H. Dong, H. Lu, L. Lu, C. Chen and W. Xiao, *Adv. Synth. Catal.* 2007, **349**, 1597-1603.
- 18 J. Kothandapani, S. M. K. Reddy, S. Thamotharan, S. M. Kumar, K. Byrappa and S. S. Ganesan, *Eur. J. Org. Chem.* 2018, 2762-2767.
- 19 B. Deka, M. L. Deb, R. Thakuria and P. K. Baruah, *Catal. Commun.*, **106**, 68-72.
- 20 B. J. P. Atienza, L. D. Jensen, S. L. Noton, A. K. V. Ansalem, T. Hobman, R. Fearn, D. J. Marchant and F. G. West, *J. Org. Chem.*, 2018, **83**, 6829-6842.
- 21 A. Bahuguna, A. Kumar, S. Kumar, T. Chhabra and V. Krishnan, *ChemCatChem*, 2018, **10**, 3121-3132.